Accepted by ApJS
Preprint typeset using LATEX style emulateapj v. 19/02/01

THE *FIRST* BRIGHT QUASAR SURVEY III. THE SOUTH GALACTIC CAP[1]

Robert H. Becker[2,3,4], Richard L. White[4,5], Michael D. Gregg[2,3],
Sally A. Laurent-Muehleisen[2,3,4], Michael S. Brotherton[3,4], Chris D. Impey[6],
Frederic H. Chaffee[7], Gordon T. Richards[8], David J. Helfand[4,9,10], Mark Lacy[2,3],
Frederic Courbin[11] & Deanne D. Proctor[3]
bob@igpp.ucllnl.org
Accepted by ApJS

ABSTRACT

We present the results of an extension of the FIRST Bright Quasar Survey (FBQS) to the South Galactic cap, and to a fainter optical magnitude limit. Radio source counterparts with SERC R magnitudes brighter than 18.9 which meet the other FBQS criteria are included. We supplement this list with a modest number of additional objects to test our completeness for quasars with extended radio morphologies. The survey covers 589 deg^2 in two equatorial strips in the southern cap. We have obtained spectra for 86% of the 522 candidates, and find 321 radio-selected quasars of which 264 are reported here for the first time. A comparison of this fainter sample with the FBQS sample shows the two to be generally similar.

Fourteen new broad absorption line (BAL) quasars are included in this sample. When combined with the previously identified BAL quasars in our earlier papers, we can discern a break in the frequency of BAL quasars with radio loudness, namely that the relative number of high-ionization BAL quasars drops by a factor of four for quasars with a radio-loudness parameter $R^* > 100$.

Subject headings: surveys — quasars: general — galaxies: active — BL Lacertae objects: general — galaxies: starburst — radio continuum: galaxies

1. INTRODUCTION

For the past five years, we have been engaged in an effort to identify the quasar content of the VLA FIRST survey. Our FIRST Bright Quasar Survey (FBQS) is motivated both by the high sensitivity and excellent astrometry provided by FIRST. To date, there have been two releases of quasars discovered by the FBQS (Gregg et al. 1996, hereafter Paper I; White et al. 2000, hereafter Paper II). Both have presented quasars found in the north Galactic cap down to a limiting E ($\sim R$) magnitude of 17.8. In this paper, we are presenting the extension of the survey to the south Galactic cap. Although the survey area in the south is considerably smaller (589 square degrees vs the 2682 square degrees covered in Paper II), we have extended the optical magnitude limit to $R = 18.9$.

Except for the fainter magnitude limit, the selection criteria used to generate the list of 522 candidates are largely the same as those used in Paper II, but with two additions designed to test our completeness to quasars with extended radio morphologies. With spectra now in hand for 86% of the candidates, we have identified 321 radio-selected quasars, of which 264 are newly discovered. In this work we present the vital statistics of the quasars and nonquasars alike and contrast this sample with the brighter quasars found previously by the FBQS.

2. THE SAMPLE

As in the previous renditions of the FBQS, the FIRST survey serves as the primary catalog (Becker, White & Helfand 1995; White, Becker, Helfand & Gregg 1997; see also the FIRST home page at http://sundog.stsci.edu). In the south Galactic cap, the sky coverage is limited to two strips of sky, one along the equator and a second some 7 to 10 degrees south of the equator. Both of these areas coincide with regions slated for coverage by the Sloan Digital Sky Survey (Gunn & Knapp 1992). In addition, a short segment was added at RA $\sim$ 2 hrs to connect the two disjoint SDSS areas. Candidate quasars were identified by comparing the FIRST survey catalog to the APM catalog of optical sources on the UK Schmidt survey of the southern sky (McMahon & Irwin 1992). The spatial dis-

[1] Based on observations obtained with the W. M. Keck Observatory, which is jointly operated by the California Institute of Technology and the University of California, and the Multiple Mirror Telescope Observatory, which is jointly operated by the University of Arizona and the Smithsonian Institution.

[2] Physics Dept., University of California–Davis
[3] IGPP/Lawrence Livermore National Laboratory
[4] Visiting Astronomer, Kitt Peak National Observatory, National Optical Astronomy Observatory
[5] Space Telescope Science Institute, 3700 San Martin Dr., Baltimore, MD 21218, rlw@stsci.edu
[6] Steward Observatory, U. Arizona
[7] W. M. Keck Observatory
[8] Astronomy & Astrophysics Center, U. Chicago
[9] Astronomy Dept., Columbia University
[10] Institute of Astronomy, Cambridge University
[11] Pontificia Universidad Catolica de Chile

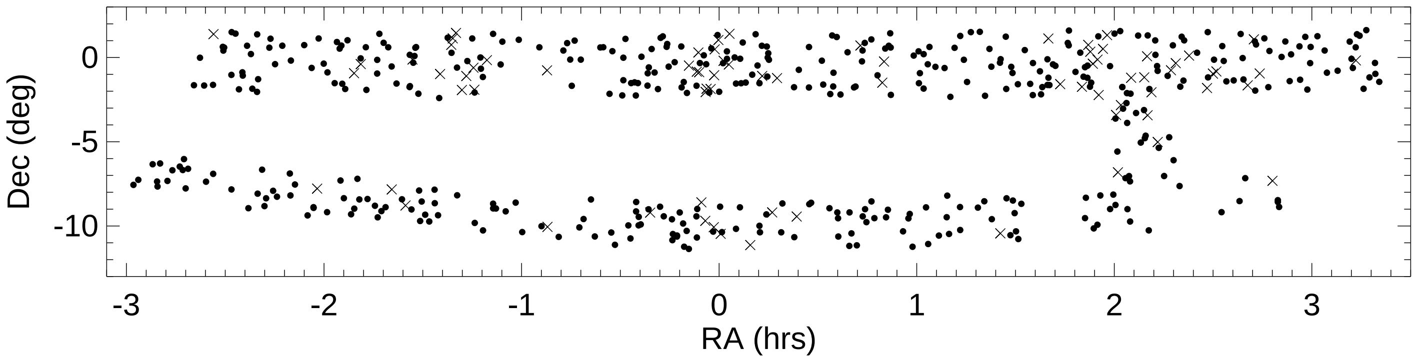

Fig. 1.— Distribution of the 522 FBQS candidates on the sky. Dots are the 447 objects with spectral identifications; x's mark the 75 objects without spectra. The gaps centered at $01^{\mathrm{h}}45^{\mathrm{m}}$ and (less obviously) at $02^{\mathrm{h}}20^{\mathrm{m}}$ result from missing SERC plate scans.

tribution of the candidates is shown in Figure 1. There are a few gaps in the coverage created where the corresponding UK Schmidt plates were never scanned by APM. The missing plates are f684 (centered at $\alpha = 1^{\mathrm{h}}42^{\mathrm{m}}$, $\delta = -10°$), f686 ($2^{\mathrm{h}}22^{\mathrm{m}}$, $-10°$), f688 ($3^{\mathrm{h}}02^{\mathrm{m}}$, $-10°$), and f760 ($3^{\mathrm{h}}02^{\mathrm{m}}$, $-5°$).

We followed many of the procedures described in detail in Paper II. Perhaps most importantly, we used the FIRST catalog positions to calculate a new astrometric solution for the UK Schmidt plates. In Paper II, we applied a plate-by-plate calibration derived from the APS catalog (Pennington et al. 1993) to the APM photometry. The APS data is limited in the southern Galactic cap, so for this paper we applied a similar photometric calibration using instead an early version, 2.1.1, of the Guide Star Catalog-II.[12] The photometric calibration used stars in the vicinity of FIRST sources rather than the FIRST optical counterparts themselves. This is important because the FBQS quasars are variable, and Malmquist bias between the APM and GSC-II epochs causes the GSC-II magnitudes for quasars to appear systematically fainter than the APM magnitudes (Helfand et al. 2001). A comparison between the GSC-II and APS magnitude calibrations in the north Galactic cap indicates excellent agreement, and we estimate that the calibrated magnitudes in this paper have an rms accuracy of $\sim 0.15^{\mathrm{m}}$ on both the R and B plates, which is similar to the uncertainties for the E and O magnitudes in Paper II.

Any optical counterpart to a FIRST radio source which met the following conditions was considered a quasar candidate:

- The radio and optical positions must coincide to better than 1.2 arcsec.
- The optical counterpart must be classified as stellar on at least one of the two plates.
- The recalibrated, extinction-corrected optical SERC R magnitude (5900–6900 Å) on the UK Schmidt red plate must be brighter than 18.9.
- The UK Schmidt color must be bluer than $B - R = 2$.

These criteria resulted in a candidate list of 505 optical counterparts. In addition, we included another seventeen candidates which failed the above criteria but represented one of the two situations described below.

If a FIRST radio source was elongated such that its radio centroid differed from the radio peak by more than 1 arcsec, the peak position was calculated and used in a second search for an optical counterpart. This resulted in the selection of another 5 candidates, 3 of which turned out to be quasars. These candidates are identified with the comment 'CJ' (core-jet) in the tables below.

In addition, for all radio doubles separated by $< 30''$ in the survey area, optical counterparts were identified along the line joining the two radio sources under the assumption that the radio double has an FR II radio morphology in which the radio flux density from the core falls below the FIRST survey limit — i.e., radio-loud quasars with extremely small core-to-lobe ratios. The positional criteria were determined from an analysis of $\sim$ 8000 optical counterparts to double radio sources in the FIRST survey (McMahon et al. 2001); we include sources within $\pm 1.5''$ of the line between the radio components and within $\pm 2''$ of the flux-weighted midpoint along the connecting line. This search added another 12 candidates to the program, of which 10 were found to be quasars. These candidates are designated with the comment 'DBL' (double) in the lists given below.

A simple search for quasars at the location of the core emission finds 96% of the radio-selected quasars. A more diligent search as outlined above finds an additional 4% of the quasars, and the majority of these are faint: for our limiting magnitude of $R = 17.8$ in the northern survey, the results here imply that we are missing less than one quasar per 100 deg^2 as a consequence of its morphology, or $\sim$ 3% of the total bright quasar population. It is worth noting that the efficiency of finding quasars with the expanded procedure (57% of the candidates turn out to be quasars) is comparable to the efficiency of searching the core positions (68% of which are quasars).

2.1. *Sample Biases*

In Paper II, we used a series of histograms and plots to illustrate the degree to which our selection criteria might be biasing the sample. For example, Figures 2a and 2b in Paper II were histograms displaying the number of quasars as a function of angular separation between the radio and optical positions and the fraction of candidates which turned

[12] Information on the GSC-II catalog is available at http://www-gsss.stsci.edu/gsc/compass/GSC2export/GSC2Export.html.

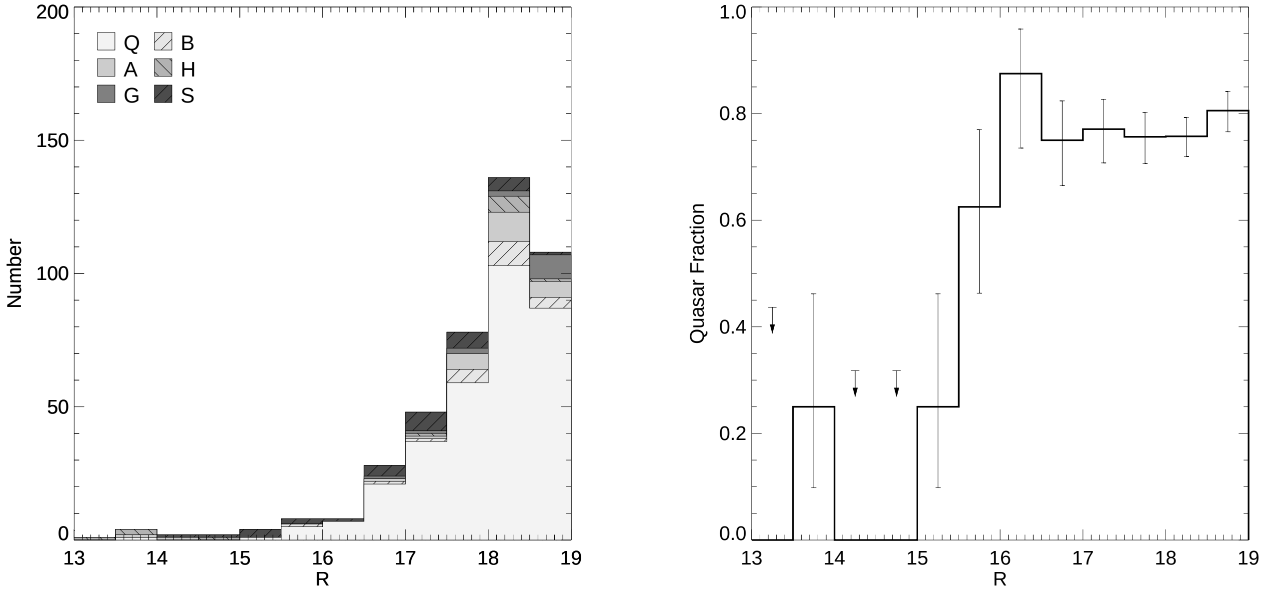

FIG. 2.— (a) A histogram of extinction-corrected SERC R magnitudes for FBQS candidates with identifications: Q=quasar, B=BL Lac object, A=narrow-line AGN, H=star-forming H II region galaxy, G=normal galaxy (no emission lines), and S=star (see §4 for details.) (b) The fraction of quasar identifications as function of R magnitude.

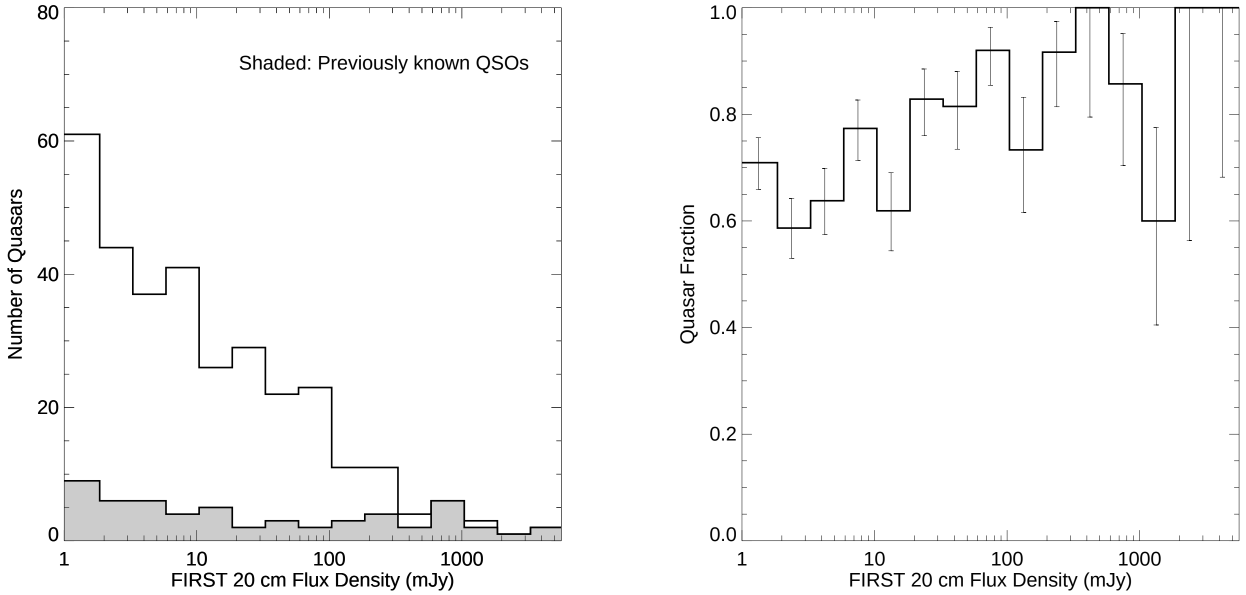

FIG. 3.— (a) A histogram of FIRST integrated radio flux densities of FBQS quasars. Shaded: previously known quasars. (b) The fraction of FBQS candidates identified as quasars as function of radio flux density. The flux densities come from the FIRST catalog and so include only the core radio emission.

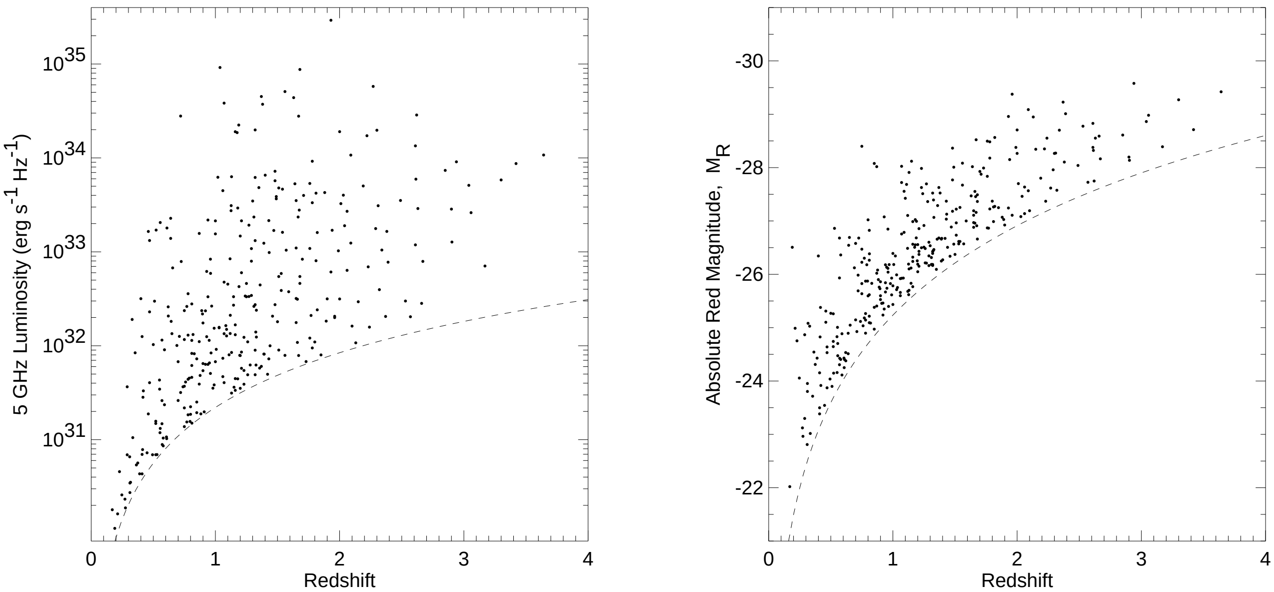

FIG. 4.— FBQS quasar luminosities versus redshift in the radio and optical. (a) Radio luminosity at a rest frequency of 5 GHz versus redshift, using spectral index $\alpha = -0.5$. (b) Absolute red magnitude versus redshift, using spectral index $\alpha_{opt} = -1$ for the K-correction. Dashed lines show the 1 mJy FIRST detection limit and the $R = 18.9$ APM magnitude limit. The radio luminosities have a much larger dynamic range and do not crowd as closely against the detection limit as do the optical magnitudes.

out to be quasars, also as a function of angular separation. The same histograms for this new sample are effectively identical; i.e., they show that very few quasars are found near the limiting separation of 1.2 arcsec. From this we still conclude that few quasars are lost due to a positional mismatch. The one obvious exception, quasars with radio jets, have now been searched for (as described above) with the result that only three additional quasars were found. While our method for going after core-jet sources is not foolproof — for example, we will still miss quasars where the jet is brighter than the core — it does suggest that these objects constitute a very small subsample of quasars.

The distribution of R magnitudes for the current sample is quite different from that of Paper II for the simple reason that we have chosen to go ~ 1.1 magnitudes fainter in the SGP. Hence the histogram of the number of quasars vs. R magnitude in Figure 2a rises sharply down to the survey limit of 19th magnitude. Figure 2b shows the success rate for finding quasars as a function of R. As in Paper II, the fraction increases with increasing magnitude before leveling off at 70% for candidates fainter than R of 16.5. The lower success rate at brighter magnitudes is largely due to optically bright galaxies which the APM catalog has misclassified as stellar.

Going deeper has not resulted in a significant difference in the color of the quasars found. As shown in Figure 5a from Paper II, most of the quasars in the previous sample have O-E between 0 and 1. The same range is applicable for the $B-R$ colors of the current sample; of candidates with $B-R > 1.5$, only 10% turn out to be quasars. There appears to be a shift of 0.1 magnitudes in the peak of the distribution (the current sample is slightly bluer), but this is possibly a consequence of the different bandpasses. Likewise a color-redshift plot for the current sample is very similar to the equivalent plot in Figure 6 of Paper II.

In Figure 3a we show a histogram of the number of quasars vs. the 20 cm radio flux density. As in Paper II, the number of quasars rises down to the flux density limit of the FIRST survey. Figure 3b demonstrates that we are nearly as efficient at finding radio-weak quasars as radio-bright quasars. In Figures 4a and 4b we show plots of radio luminosity and absolute R magnitude vs. redshift. The radio luminosity plot is virtually indistinguishable from Figure 8a in Paper II, an unsurprising result given that both samples have the same radio flux density limit. The plot of M_R (Fig. 4b) is strikingly different since here we are going 1.1 magnitudes deeper over a much smaller area. In this sample there is a relative paucity of very luminous quasars and a much stronger representation of lower luminosity quasars.

3. OPTICAL SPECTROSCOPY

Spectra were collected at a variety of observatories, including the Lick Shane 3-m telescope, the 'classic' MMT (6×1.8-m), the 10-m Keck-II Observatory, and the ESO 3.6-m telescope. Instrument parameters for the first three observatories are given in Table 1 of Paper II; for the ESO 3.6-m, we used the EFOSC2 (ESO Faint Object Spectrograph and Camera). The observations were made without regard to atmospheric transparency or seeing, so the flux calibration of the resulting spectra are not absolute. Where possible, the slit was oriented at the parallactic angle to minimize differential slit losses. Since the data were taken at a number of different sites with dissimilar spectrographs, the resolution and wavelength coverage are not uniform. In all cases the spectra were reduced using standard IRAF routines.

4. SPECTROSCOPIC RESULTS

Spectra were obtained (or identifications determined from the literature) for 447 of the 522 quasar candidates, and were classified using the same conventions described in detail in Paper II. Briefly, we classified spectra as quasars if there were any broad emission lines with rest-frame equivalent widths greater than 5 Å; objects with weaker broad lines were classified as BL Lacs. We classified a spectrum as a narrow-line AGN if narrow lines were present in the spectra with ratios consistent with those expected for an AGN (i.e., [O III]λ5007/Hβ greater than 3 or [N II]λ6583/Hα greater than 0.6). Any spectra with narrow lines failing to meet these criteria were classified as H II/star-forming galaxies. Spectra with very weak or no emission lines were classified as normal galaxies, unless the Ca H & K 4000 Å break was less than 25% in which case they were assigned a classification of BL Lac. Spectra at zero redshift were deemed stars. In all, the distribution of objects was 321 quasars, 23 BL Lac, 31 AGN, 23 starburst, 17 normal galaxies, and 32 stars. The latter are roughly consistent with the expected chance coincidence rate (although a few are real detections of stellar radio sources – see Helfand et al. 1999); note that the putative double radio sources are overrepresented by a factor of ~ 3 in the stellar list, consistent with the factor of ~ 3 increase in the accepted matching area (12 arcsec^2 vs. 4.5 arcsec^2).

The fractions of the sample that are narrow-line AGN, BL Lacs, and normal galaxies are all roughly consistent with the fractions derived in our sample limited to $R \leq 17.8$. The fraction of H II galaxies, however, is lower by a factor of 3.5, a result of the fainter optical magnitude limit of this sample. The radio flux densities of most of the star-forming galaxies are very close to the FIRST threshold (85% have $S_p < 3.0$ mJy). For a constant radio-to-optical flux ratio, lowering the optical magnitude limit by 1.2 magnitudes would render most of these objects undetectable. Finally, the fraction of quasars is considerably higher in this fainter sample, reflecting their steep $N(m)$ distribution.

In Tables 1–6 we list all the candidates with spectroscopic classifications. For each object we include the FIRST catalog RA and Dec (J2000), the recalibrated and extinction-corrected R and B magnitudes, the red extinction correction $A(R)$, and the FIRST peak and integrated radio flux densities. The radio-optical positional separation and APM star-galaxy classification (used to define the sample) are also given. The objects have been segregated into 6 tables by their optical spectral classification. Quasars are listed in Table 1, narrow line AGN in Table 2, BL Lac objects in Table 3, H II/star-forming galaxies in Table 4, galaxies without strong emission lines in Table 5, and stars in Table 6. Table 7 lists the objects for which spectra have not yet been obtained.

In Tables 1–5, we list the measured redshift (except for the 2/3 of the BL Lacs for which none was derivable from the spectrum). We use the redshift to calculate for each object the radio luminosity L_R at a rest frequency of 5 GHz (assuming a radio spectral index of -0.5), the absolute B magnitude M_B, and, as a measure of radio loudness, the ratio R^* of the 5 GHz radio flux density to the 2500 Å optical flux in the quasar rest frame (assuming an optical spectral index of -1 and the definition given by Stocke et al. 1992). The cosmological parameters $H_0 = 50\,\mathrm{km\,s^{-1}Mpc^{-1}}$, $\Omega = 1$, and $\Lambda = 0$ were used for the luminosity calculations. There is also a comment column, which notes the details of particular interest such as whether objects were selected as core-jet or double sources, the presence of broad absorption lines (BALs) or damped Lyman alpha absorption lines, whether the object was previously known or, in NED, associated with a ROSAT or IRAS source.

The spectra for all the objects identified as quasars are displayed in the figure at the end of the paper.

5. DISCUSSION

This new quasar sample contains half as many quasars as presented in Paper II. This is in part a reflection of two competing factors; a reduced survey area (600 square degrees vs. 2700 square degrees) and a fainter magnitude limit ($R = 18.9$ vs. $E = 17.8$). If we restrict the comparison to quasars brighter than $R = 17.8$ and normalize for the area surveyed, we still find a unexpectedly small number of quasars in the new sample. For example, the areal densities (quasars per deg^2) of quasars with $R < 17.8$ and $0.3 < z < 2.2$ in Paper II and this paper are 0.203 and 0.149 respectively, i.e., this paper has 27% fewer bright quasars than expected based on Paper II. This difference is significant at the 2.9 sigma level. Since quasars have a very steep number/magnitude relation, even a small systematic error in the photometry of the two samples could account for much of the discrepancy. In fact, the entire effect could arise if this paper magnitudes were only 0.15 magnitudes too faint. Although we don't believe the systematic errors are that large, even an error of 0.1 magnitudes could reduce the discrepancy to below 2 sigma.

Of course, the radio flux density limits for Paper II and this paper are nominally the same. Since the radio loudness is defined in terms of the ratio of radio to optical luminosity, the extra quasars found by going to fainter optical limits are, on average, more radio-loud. This can be seen in Figure 5 which shows a histogram of the number of quasars as a function of radio loudness. The histogram peaks at R^* greater than 10, whereas in the previous sample (see Fig. 15a in Paper II) the equivalent histogram peaks at 5. Therefore differences between the two samples will, in part, reveal factors that depend on radio loudness. Going to fainter optical magnitudes does not appreciably increase our sensitivity to nearby quasars because the rapid evolution of quasars means there are few nearby quasars to discover, and very low-luminosity, nearby quasars will not look stellar and hence do not get into the survey. Consequently, it is not surprising that this new sample tends to select a more distant set of quasars. In Figure 6 we show the histogram of the quasar redshifts. While in Paper II this distribution was flat between redshifts of 0–1.2 (see Fig. 12 in Paper II), this sample shows a significant decline for redshifts below 0.7.

One attribute of quasars which appears to correlate with radio-loudness is the likelihood of broad absorption lines (BALs) in a quasar spectrum. For a long time, it was thought that BALs only occur in radio-quiet quasars (Stocke et al. 1992). More recently, quasar searches based on the FIRST and NVSS radio surveys have found a number of radio-loud BAL quasars (Becker et al. 1997; Brotherton et al. 1998; Becker et al. 2000). However, the size of

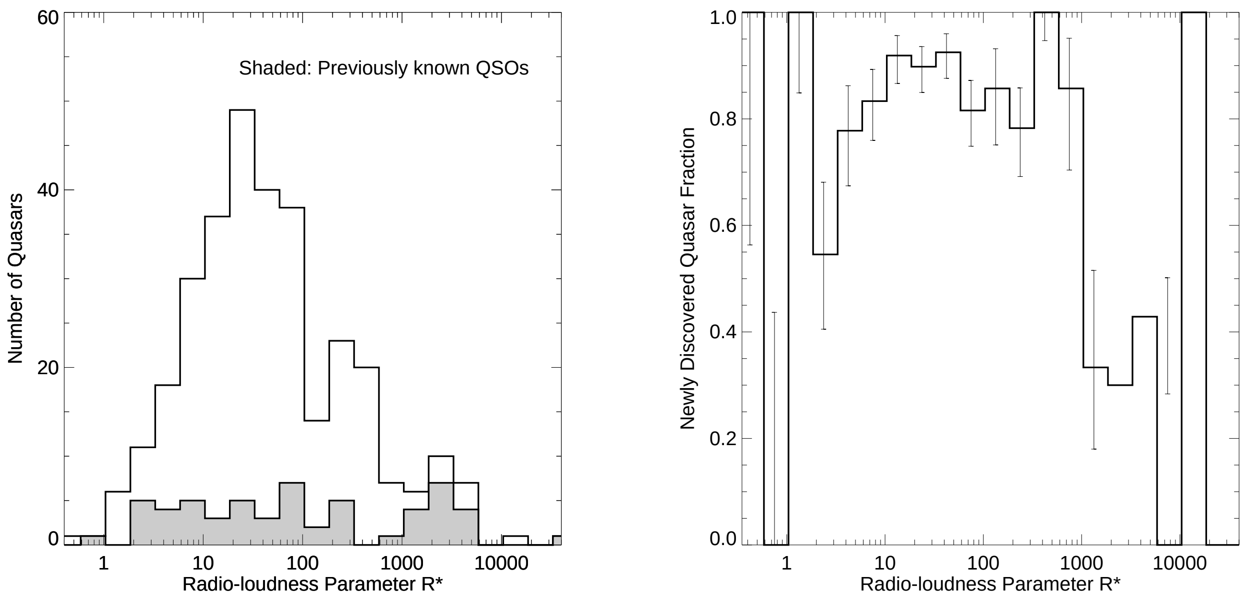

FIG. 5.— (a) A histogram of radio-optical ratio R^* (Stocke et al. 1992) for FBQS quasars. Shaded: previously known quasars. (b) The fraction of quasars that were newly discovered versus R^*. The FBQS is increasing the number of known objects in the radio-quiet/radio-loud transition region ($R^* = 1$–100) by a large factor.

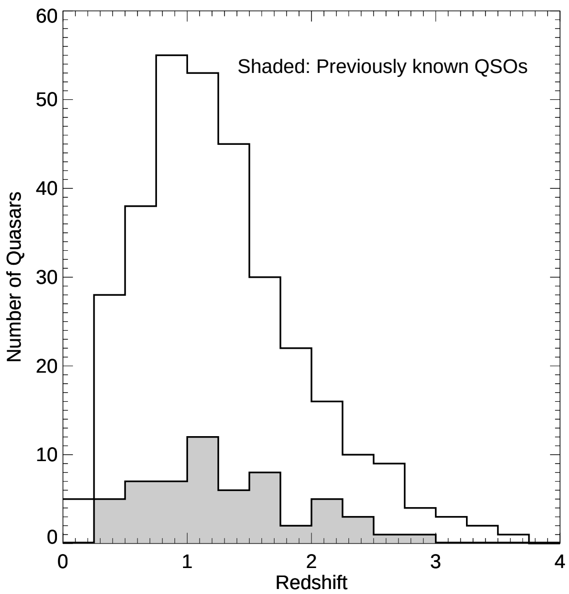

FIG. 6.— Histogram of redshifts for FBQS quasars. Shaded: previously known quasars.

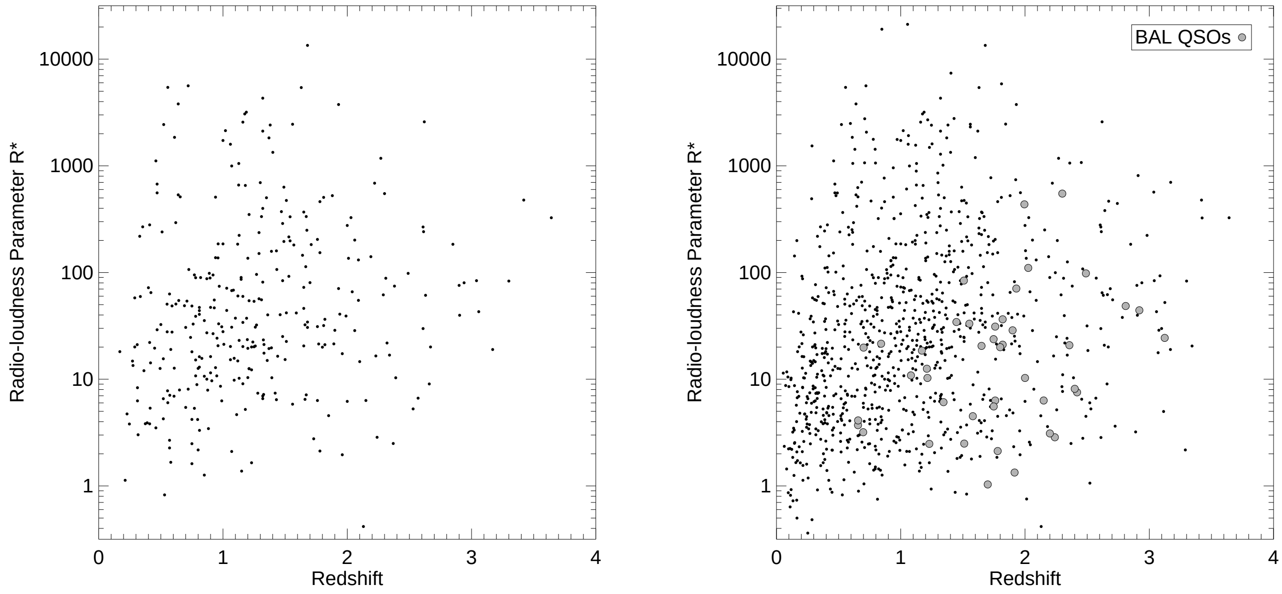

FIG. 7.— Radio-optical ratio R^* (rest-frame ratio of the 5 GHz radio flux density to the 2500 Å optical flux; Stocke et al. (1992)) versus redshift for FBQS quasars. (a) Quasars from this paper. (b) Quasars from this paper combined with those from Paper II. Broad-absorption line quasars are indicated; they are evidently more common among quasars with $R^* < 100$ than among the radio-louder objects.

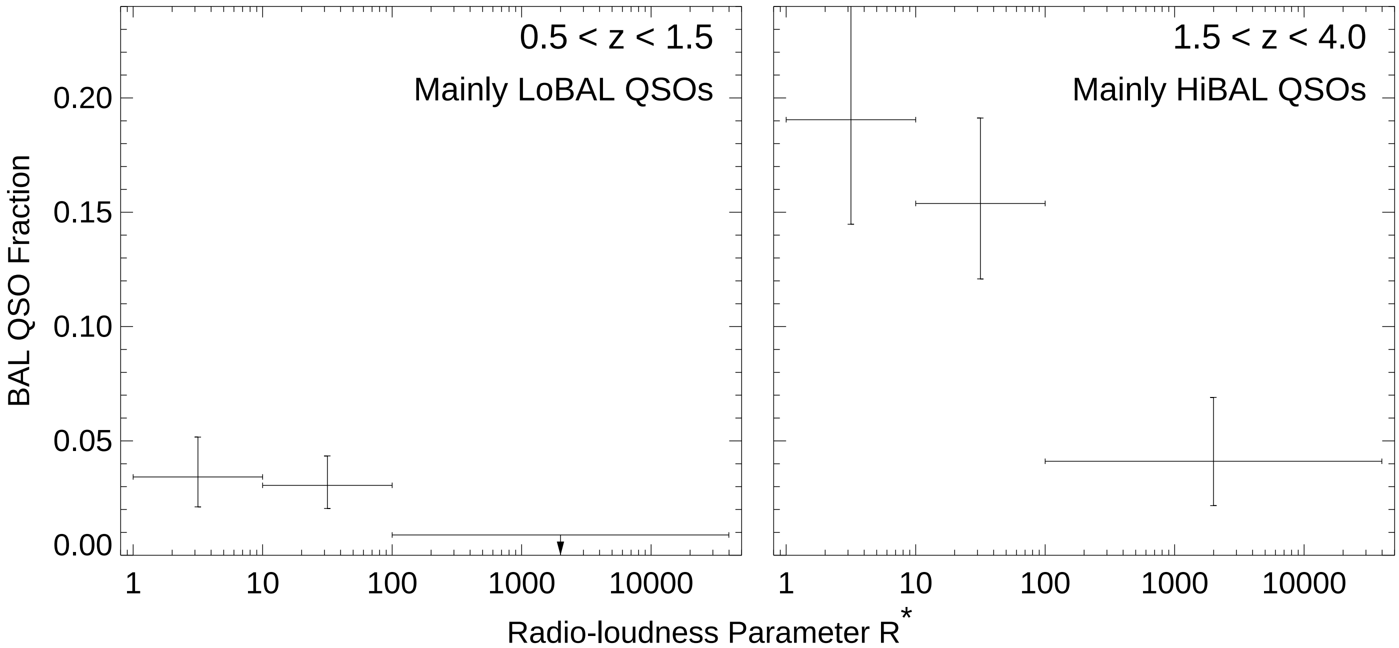

FIG. 8.— The fraction of BAL quasars as a function of radio-loudness for the combined samples from this paper and Paper II. The left panel shows the distribution of 12 BAL QSOs (11 LoBALs, 1 HiBAL) among 507 quasars with $0.5 < z < 1.5$. The right panel the distribution of 31 BAL QSOs (6 LoBALs, 25 HiBALs) among the 245 quasars with $z > 1.5$. The error bars show the uncertainty in the BAL fraction computed from the binomial distribution. Low BALnicity objects classified as 'BAL?' are included; if they were excluded, the plotted points for the R^* =10–100 bins and the $R^* > 100$ bin in the right panel would shift downward by $\sim 1/2\sigma$. The BAL quasar R^* distribution differs from that for the non-BAL quasars at greater than 99% confidence for the $z > 1.5$ sample.

the samples has limited our ability to quantify how BAL frequency depends on radio-loudness. With this sample, it is worth revisiting this question. In Figure 7(b) we plot radio-loudness vs. redshift for the combined samples from this work and Paper II. The BALs are highlighted in the figure. It is clear from the figure that the BALs straddle the radio-loud/radio-quiet divide but do not seem to occur as often in the most radio-loud segment of the population.

The classification of quasars as BAL QSOs is somewhat problematic. One approach is to calculate a 'BALnicity' index following the prescription of Weymann et al. (1991), although in many ways this approach is too conservative (Becker et al. 2000). Table 8 gives the BALnicity indices for all our candidate BAL quasars; those with zero BALnicity values (that we nonetheless believe are likely to be BAL QSOs) are classified as 'BAL?'. Believing in a democratic approach, we show all the spectra in the sample in Figure 9 so the reader can see for herself the features we are willing to call BALs. The figure also serves other purposes since many other phenomena are present in quasar spectra.

Figure 8 shows the fraction of BAL quasars (including 4 objects classified as 'BAL?') as a function of radio-loudness for the combined samples from Paper II and this paper. If the 'BAL?' objects were excluded, the plotted points would shift by less than the error bars. In examining Figures 7 and 8, it is worthwhile to note that there are three distinct types of BAL quasars: high ionization objects (HiBALs) that show broad absorption from C IV and Si IV; low ionization objects (LoBALs) that, in addition to C IV and Si IV, also show absorption due to Mg II and occasionally Al III $\lambda1858$; and a rare class of LoBALs (FeLoBALs) that show superposed absorption from metastable excited states of Fe II. Since C IV does not move into our spectral window for $z < 1.5$, identified HiBALs are limited to redshifts greater than 1.5. So while some of the low redshift quasars may be HiBALs, they cannot be recognized as such. Likewise some of the $z > 1.5$ HiBALs might actually be LoBALs or FeLoBALs but since Mg II is shifted into the near IR at these redshifts, they cannot be so identified unless absorption by Al III is also present. For the most part, the fraction of BALs found among $z > 1.5$ quasars can be taken as a proxy for the fraction of HiBALs. And by the same token, the fraction of quasars showing BALs in the redshift range of 0.5–1.5 can be taken as a proxy for the fraction of LoBALs.

In Becker et al. (2000), we found the fraction of quasars which are HiBALs and LoBALs (including FeLoBALs) among radio-selected quasars with $R < 17.8$ to be 18% and 3% respectively. If we combine the current sample with those from Paper II and consider only quasars with a radio-loudness parameter $R^* < 100$, we get very similar numbers (17% and 3%; see Fig. 8). But for quasars with $R^* > 100$ the fraction of HiBALs and LoBALs drops to 4% and $< 1.5\%$ respectively. (If the low-BALnicity 'HiBAL?' objects are omitted, the fraction of $R^* > 100$ quasars that are HiBALs drops to 3%.) While the apparent drop in the fraction of LoBALs among the most radio-loud quasars is not statistically significant (due to the small number of quasars that are LoBALs), the decrease in HiBALs is significant. We can rule out at 98.9% confidence the hypothesis that the $R^* < 100$ and $R^* > 100$ BAL fractions are the same for the $z > 1.5$ sample. A two-sided Kolmogorov-Smirnov test (Press et al. 1992) indicates the probability that the $z > 1.5$ BAL and non-BAL quasars have the same R^* distribution is only 0.0053.

6. EDITORIAL

The utility of quasar surveys has evolved with time. Today, with well over 10,000 quasars in the literature and many more to appear soon, the rationale for doing surveys is quite different than in the past. The need for ever larger surveys is being driven by the desire either to find large numbers of rare quasars or to nail down subtle correlations between quasar properties with massive numbers. As an example of the former, with this addition to the FBQS we are just beginning to discern the dependence of the BAL phenomena on radio-loudness. The fact is that current samples are still not large enough to provide quantities of very rare classes of quasars sufficient for reliable statistical analyses. Other areas of quasar research that are still limited by current sample size are gravitational lensing, the frequency and nature of damped Lyman alpha absorbers, the frequency and longevity of binary quasars, and quasar large-scale structure. Perhaps in five years when the SDSS 100,000 quasars and the 2dF 30,000 quasars are publically available, we may finally stop searching for more quasars. But we sincerely doubt it.

We acknowledge extensive use of the NASA/IPAC Extragalactic Database (NED), which is operated by the Jet Propulsion Laboratory, Caltech, under contract with the National Aeronautics and Space Administration. The success of the FIRST survey is in large measure due to the generous support of a number of organizations. In particular, we acknowledge support from the NRAO, the NSF (grants AST-98-02791 and AST-98-02732), the Institute of Geophysics and Planetary Physics (operated under the auspices of the U.S. Department of Energy by Lawrence Livermore National Laboratory under contract No. W-7405-Eng-48), the Space Telescope Science Institute, the National Geographic Society (grant NGS No. 5393-094), and Columbia University. F. Courbin acknowledges financial support from Chilean grant FONDECYT/3990024 and additional support from the European Southern Observatory.

REFERENCES

Becker, R. H., White, R. L., & Helfand, D. J. 1995, ApJ, 450, 559
Becker, R. H., Gregg, M. D., Hook, I. M., McMahon, R. G., White, R. L., & Helfand, D. J. 1997, ApJ, 479, L93
Becker, R. H., White, R. L., Gregg, M. D., Brotherton, M. S., Laurent-Muehleisen, S. A., & Arav, N. 2000, ApJ, 538, 72
Brotherton, M. S., van Breugel, W., Smith, R. J., Boyle, B. J., Shanks, T., Croom, S. M., Miller, L., & Becker, R. H. 1998, ApJ, 505, L7
Gregg, M., D., Becker, R. H., White, R. L., Helfand, D. J., McMahon, R. G., & Hook, I. M. 1996, AJ, 112, 407 (Paper I)
Gunn, J. E., & Knapp, G. R. 1992, PASP, 43, 267

Helfand, D. J., Schnee, S., Becker, R. H., White, R. L., & McMahon, R. G. 1999, AJ, 117, 1568
Helfand, D. J., Stone, R. P. S., Willman, B., White, R. L. Becker, R. H., Price, T., Gregg, M. D., & McMahon, R. G. 2001, AJ, in press
McMahon, R. G., & Irwin, M. J. 1992, in Digitised Optical Sky Surveys, eds. H. T. MacGillivray and E. B. Thomson (Dordrecht: Kluwer), p. 417
McMahon, R. G., White, R. L., Helfand, D. J., & Becker, R. H. 2001, ApJS, in press
Moshir, M. M., et al. 1992, Explanatory Supplement to the IRAS Faint Source Survey, Version 2, JPL D-10015 (Pasadena: JPL)
Pennington, R. L., Humphreys, R. M., Odewahn, S. C., Zumach, W., & Thurmes, P. M. 1993, PASP, 105, 521
Press, W. H., Teukolsky, S. A., Vetterling, W. T., & Flannery, B. P. 1992, Numerical Recipes in C, 2nd Edition (Cambridge: Cambridge University Press)
Schlegel, D. J., Finkbeiner, D. P., & Davis, M. 1998, ApJ, 500, 525
Stocke, J. S., Morris, S. L., Weymann, R. J., & Foltz, C. B. 1992, ApJ, 396, 487
Véron-Cetty, M.-P., & Véron, P. 1998, A Catalogue of Quasars and Active Nuclei (8th Edition), European Southern Observatory Scientific Report, 18, 1
Voges, W. et al. 1996, IAU Circ., 6420
Weymann, R. J., Morris, S. L., Foltz, C. B., & Hewett, P. C. 1991, ApJ, 373, 23
White, R. L., Becker, R. H., Helfand, D. J., & Gregg, M. D. 1997, ApJ, 475, 479
White, R. L., Becker, R. H., Gregg, M. D. Laurent-Muehleisen, S. A., et al. 2000, ApJS, 126, 133 (Paper II)

Table 1
FIRST Bright Quasar Catalog

RA (1)	Dec (2)	Cl (3)	R (4)	B (5)	B-R (6)	A(R) (7)	Sep (8)	S_p (9)	S_i (10)	M_B (11)	$\log L_R$ (12)	$\log R^*$ (13)	z (14)	Notes (15)
21 02 08.142	-07 33 34.62	*	18.02	19.01	0.99	0.21	0.72	1.94	1.95	-27.6	32.5	0.96	2.660	
21 07 57.680	-06 20 10.52	*	16.64	18.02	1.38	0.17	0.34	19.21	19.61	-25.2	32.3	1.74	0.644	
21 09 18.684	-07 21 37.99	*	18.23	20.15	1.92	0.30	0.45	1.18	0.69	-24.6	31.6	1.30	1.230	
21 09 26.412	-07 39 25.92	*	18.69	19.62	0.93	0.23	0.80	44.85	57.14	-26.1	33.6	2.72	1.880	
21 10 13.184	-06 17 20.85	*	18.28	19.66	1.39	0.22	0.23	32.89	36.21	-25.5	33.2	2.57	1.470	
21 17 28.905	-06 01 49.02	*	17.76	18.20	0.43	0.35	0.64	78.43	81.04	-27.4	33.7	2.31	1.760	
21 18 43.248	-06 36 17.94	*	16.60	17.92	1.32	0.37	0.39	75.52	77.44	-23.7	32.3	2.34	0.330	X
21 23 36.041	-01 39 47.38	gR	18.53	19.36	0.83	0.13	0.19	1.26	1.21	-23.2	30.8	1.10	0.494	X
21 24 10.271	-07 22 19.95	*	17.10	17.88	0.78	0.33	0.87	13.96	16.46	-27.7	33.0	1.49	1.760	HiBAL
21 26 17.353	-01 37 26.29	*	18.44	19.24	0.79	0.14	0.27	9.80	11.58	-25.3	32.5	1.94	1.146	
21 26 20.135	-06 54 19.23	*	16.79	17.57	0.77	0.27	12.41	7.22	7.10	-24.6	31.5	1.15	0.417	DBL
21 29 16.616	+00 37 57.02	*	17.27	17.86	0.58	0.12	0.32	49.10	51.98	-29.0	34.0	1.90	2.940	dmpLα
21 31 53.677	-07 49 53.01	*	18.45	18.77	0.32	0.09	0.34	12.28	13.53	-27.2	33.1	1.74	2.090	
21 33 07.655	+01 25 05.07	*	15.15	15.51	0.36	0.15	1.57	1.89	9.30	-28.0	32.1	0.40	0.750	CJ
21 35 13.133	-00 52 44.08	*	17.91	18.54	0.63	0.12	0.46	1.84	1.32	-26.9	32.0	0.81	1.660	o
21 36 38.600	+00 41 54.47	*	16.87	17.24	0.37	0.18	0.32	3546.71	3712.01	-28.6	35.5	3.57	1.930	o,X
21 37 02.755	-08 56 41.25	*	17.19	18.09	0.90	0.09	0.09	79.29	81.03	-27.1	33.6	2.29	1.490	
21 37 48.433	+00 12 19.84	*	18.01	18.32	0.31	0.17	0.11	36.02	39.56	-27.1	33.4	2.05	1.666	
21 38 13.749	-01 51 07.46	*	18.10	19.02	0.93	0.13	0.15	28.94	28.84	-25.1	32.8	2.27	0.961	
21 39 39.513	-02 02 26.13	gR	18.07	19.34	1.27	0.13	0.18	1.39	0.91	-21.9	30.4	1.17	0.272	
21 39 42.508	+01 22 27.59	*	18.77	19.46	0.69	0.13	0.28	147.75	154.22	-25.6	33.8	3.13	1.401	
21 40 00.161	-01 17 14.02	*	18.60	18.61	0.02	0.14	0.21	6.95	7.12	-25.6	32.2	1.49	0.990	
21 41 11.893	-06 39 30.67	*	18.66	18.73	0.06	0.10	0.29	4.71	5.07	-24.1	31.5	1.44	0.551	
21 42 25.329	-08 21 22.77	*	16.97	17.01	0.04	0.11	0.90	2.03	1.79	-25.9	31.2	0.36	0.570	
21 43 24.372	+00 35 02.94	*	18.87	19.37	0.50	0.18	0.24	45.22	46.28	-26.6	33.6	2.51	2.030	
21 44 32.747	-07 54 42.74	gR	18.41	19.51	1.10	0.11	0.06	56.32	60.53	-26.2	33.6	2.70	1.810	
21 49 37.443	-06 53 12.23	*	18.75	19.56	0.81	0.11	1.19	13.05	19.68	-25.8	33.0	2.26	1.570	
21 49 48.171	-08 11 16.18	gB	17.12	16.18	-0.94	0.10	0.29	1.13	0.65	-29.9	32.0	-0.38	2.130	
21 49 56.740	-00 10 51.95	*	18.64	18.91	0.27	0.41	0.14	7.82	7.73	-24.8	32.1	1.67	0.810	
21 51 11.196	-07 32 20.04	*	18.31	19.90	1.59	0.13	0.27	1.41	1.48	-25.1	31.8	1.29	1.370	
21 53 59.827	+00 44 13.32	*	18.59	19.07	0.47	0.19	0.51	6.73	6.48	-25.2	32.2	1.64	1.030	
21 55 01.482	-09 22 24.66	*	13.87	14.13	0.26	0.12	0.25	1.39	1.17	-26.2	30.1	-0.90	0.190	
21 56 48.431	-08 53 08.37	*	18.75	19.32	0.56	0.09	0.36	2.54	2.33	-26.5	32.3	1.24	1.960	
21 58 22.487	+01 07 49.67	*	18.48	18.80	0.32	0.14	0.95	1.21	1.02	-24.1	30.9	0.85	0.572	
21 59 54.456	-00 21 50.34	*	16.49	16.98	0.50	0.16	0.15	2.46	2.17	-28.9	32.3	0.29	1.960	
22 00 56.352	-09 10 50.95	*	17.82	18.40	0.58	0.11	0.91	1.11	1.06	-25.3	31.2	0.62	0.796	
22 01 03.119	-00 52 59.68	*	15.65	16.38	0.74	0.20	0.83	1.47	1.58	-24.3	30.2	0.05	0.213	X
22 03 14.811	-01 31 23.37	*	16.52	16.28	-0.24	0.33	0.30	14.21	14.25	-26.9	32.1	0.90	0.650	
22 03 55.563	+00 55 16.75	*	17.76	18.10	0.34	0.13	0.11	2.75	2.49	-25.3	31.5	0.91	0.720	X
22 05 16.310	+00 42 30.14	*	18.50	19.62	1.12	0.15	0.22	6.35	5.80	-24.8	32.2	1.83	1.084	
22 06 25.990	-01 52 01.12	*	16.80	17.54	0.74	0.51	0.38	2.60	2.97	-26.9	31.9	0.67	1.110	
22 07 08.347	+01 01 25.62	*	18.62	19.02	0.40	0.14	0.24	15.65	16.74	-27.8	33.5	1.88	2.900	
22 08 13.661	-09 18 19.55	*	17.57	18.22	0.66	0.11	0.90	1.01	1.06	-27.3	31.8	0.44	1.730	
22 09 11.432	-08 58 17.25	*	18.24	19.27	1.03	0.11	0.23	16.52	17.03	-24.8	32.5	2.14	0.940	
22 10 08.888	-07 12 04.30	*	18.36	18.79	0.43	0.16	0.61	1.27	1.67	-25.4	31.5	0.93	0.980	
22 12 52.576	-01 55 18.72	gR	18.26	19.50	1.24	0.28	0.33	1.09	1.01	-21.7	30.3	1.13	0.276	
22 13 13.145	-08 23 55.80	*	18.32	19.60	1.29	0.12	0.47	5.79	6.65	-24.7	32.2	1.85	1.030	
22 15 28.225	-08 48 00.25	*	18.74	19.20	0.45	0.15	0.93	1.36	1.25	-24.4	31.3	1.03	0.780	
22 16 08.890	-00 57 08.34	*	17.34	17.80	0.46	0.25	0.05	6.56	6.30	-28.6	32.9	1.01	2.390	
22 16 18.445	-09 29 13.34	*	18.51	18.92	0.41	0.17	0.71	1.21	1.30	-26.0	31.7	0.84	1.320	
22 16 48.628	+01 24 27.32	*	18.85	19.31	0.46	0.12	1.07	20.20	30.29	-26.7	33.4	2.30	2.060	
22 18 06.679	+00 52 23.98	*	17.11	17.70	0.58	0.16	0.20	53.42	54.77	-27.1	33.3	1.98	1.270	
22 18 41.898	-08 53 05.67	*	17.72	17.90	0.18	0.15	0.32	1.74	1.59	-25.6	31.3	0.62	0.750	
22 19 30.426	+00 36 26.81	*	18.41	19.49	1.08	0.16	0.42	2.53	2.39	-25.2	31.9	1.37	1.196	
22 20 32.254	-00 31 57.24	*	18.81	19.51	0.70	0.21	0.41	4.49	4.35	-25.6	32.3	1.60	1.460	
22 22 01.478	-01 32 43.38	*	18.37	18.94	0.57	0.24	6.34	24.88	29.53	-26.1	33.1	2.20	1.390	DBL
22 26 06.033	-01 41 57.22	gR	18.11	18.78	0.67	0.13	0.18	2.74	1.77	-21.3	30.3	1.26	0.170	
22 27 29.086	+00 05 22.19	*	18.26	18.86	0.59	0.20	0.28	91.64	97.51	-26.4	33.7	2.68	1.510	
22 27 44.588	+00 34 50.83	*	18.66	19.14	0.48	0.17	0.15	30.53	31.64	-26.1	33.2	2.30	1.540	
22 28 40.040	-02 08 56.23	*	18.62	18.72	0.10	0.13	0.32	1.30	1.08	-24.3	31.0	0.84	0.606	
22 28 52.605	-07 53 46.53	*	18.28	18.28	-0.00	0.13	0.22	130.09	151.83	-24.9	33.1	2.73	0.640	
22 29 12.231	-09 42 18.97	gR	18.10	18.45	0.35	0.14	0.37	7.10	11.62	-24.5	32.0	1.69	0.590	
22 29 40.075	-08 32 54.44	*	17.64	18.16	0.52	0.14	0.19	939.91	972.84	-27.2	34.7	3.39	1.560	o
22 30 43.748	-09 19 51.37	*	18.46	18.94	0.48	0.16	0.25	3.19	3.22	-26.0	32.1	1.24	1.330	
22 31 58.211	-09 43 59.51	*	16.98	17.58	0.59	0.14	0.51	30.27	32.36	-26.5	32.8	1.74	0.930	
22 33 34.900	-07 50 43.17	*	17.73	18.41	0.69	0.13	0.16	47.33	48.68	-26.7	33.3	2.20	1.430	
22 33 38.667	-08 38 53.18	*	17.59	17.95	0.36	0.14	0.36	9.20	8.84	-28.3	33.0	1.23	2.340	
22 34 38.132	-09 21 46.39	gR	16.92	17.53	0.62	0.16	1.00	1.51	1.87	-23.4	30.4	0.58	0.247	
22 34 58.757	-02 24 18.89	*	17.99	19.13	1.14	0.14	0.07	6.36	6.06	-23.7	31.6	1.70	0.550	
22 37 34.133	+01 10 35.47	*	17.94	18.30	0.36	0.21	0.67	1.02	1.14	-24.4	30.8	0.63	0.520	o
22 38 43.573	+00 16 48.15	*	18.51	20.21	1.70	0.17	0.15	36.26	37.54	-27.0	33.9	2.68	3.420	
22 40 23.264	-00 35 55.75	*	18.27	19.01	0.74	0.14	0.25	5.67	5.36	-25.6	32.2	1.53	1.160	
22 40 26.795	-08 10 42.28	*	17.69	18.50	0.82	0.11	0.37	11.07	10.89	-26.5	32.6	1.60	1.360	
22 43 31.941	-00 12 32.51	*	18.50	18.45	-0.04	0.17	0.35	21.40	21.67	-27.5	33.3	1.82	2.040	
22 45 00.822	+01 07 48.47	*	18.11	19.42	1.31	0.22	1.03	1.31	0.75	-24.3	31.3	1.10	0.800	
22 45 43.741	-02 04 41.98	*	17.94	19.26	1.32	0.16	6.08	240.59	271.76	-25.0	33.8	3.33	1.020	DBL
22 45 47.147	-09 49 07.72	gR	18.27	19.06	0.79	0.12	0.04	7.80	8.33	-23.1	31.5	1.81	0.420	
22 47 39.353	-00 39 53.46	*	16.68	17.31	0.63	0.25	0.77	1.54	1.58	-26.4	31.4	0.34	0.800	o
22 48 17.530	-10 15 46.99	*	16.47	16.83	0.36	0.13	0.09	18.23	19.22	-24.5	31.6	1.30	0.290	
22 51 21.367	-08 40 34.78	*	17.69	17.93	0.24	0.11	0.26	21.34	21.24	-27.9	33.2	1.61	1.940	

Table 1—*Continued*

RA (1)	Dec (2)	Cl (3)	R (4)	B (5)	B-R (6)	A(R) (7)	Sep (8)	S_p (9)	S_i (10)	M_B (11)	$\log L_R$ (12)	$\log R^*$ (13)	z (14)	Notes (15)
22 53 39.114	-00 24 47.50	*	18.60	18.39	-0.21	0.24	0.17	15.49	15.77	-24.5	32.1	1.80	0.570	
22 54 09.587	+00 56 28.69	*	16.45	17.16	0.71	0.27	0.67	1.25	0.60	-27.4	31.6	0.14	1.150	
22 55 10.686	-09 07 58.54	*	18.64	19.15	0.51	0.10	5.84	15.97	33.07	-23.0	32.1	2.45	0.410	DBL
22 58 12.231	-08 36 49.67	gR	18.57	19.37	0.81	0.10	0.06	27.89	30.18	-23.7	32.4	2.47	0.620	
22 59 08.398	+01 03 11.42	*	18.50	19.03	0.53	0.15	0.13	9.39	9.48	-25.8	32.5	1.75	1.290	
23 00 11.749	-10 21 44.02	*	17.99	18.50	0.52	0.11	0.24	166.18	179.27	-27.7	34.3	2.74	2.300	HiBAL?
23 05 24.747	+00 36 24.68	gR	18.80	19.42	0.62	0.13	0.73	1.24	1.03	-23.6	31.0	1.10	0.608	
23 12 41.768	+00 24 50.58	*	18.75	19.59	0.84	0.13	0.27	1.92	2.41	-26.2	32.3	1.33	1.892	
23 13 50.527	+00 51 17.84	*	18.57	19.24	0.66	0.12	0.80	2.57	3.39	-24.8	31.8	1.43	0.920	
23 14 46.506	-00 07 17.13	gR	18.40	19.23	0.83	0.11	0.15	2.93	3.01	-24.3	31.6	1.39	0.739	
23 15 14.859	-01 40 47.25	*	18.41	19.15	0.75	0.11	0.18	1.14	0.64	-25.9	31.7	0.87	1.420	
23 16 07.226	+01 00 13.56	*	17.73	18.45	0.72	0.12	0.32	89.57	96.19	-28.1	34.1	2.43	2.610	
23 17 33.166	-10 05 04.11	*	18.87	19.30	0.43	0.08	0.43	3.02	2.47	-23.7	31.4	1.44	0.590	
23 17 59.628	-00 07 33.12	*	18.73	19.51	0.78	0.12	0.15	8.64	9.41	-25.1	32.4	1.95	1.146	
23 21 04.650	-08 25 36.81	gB	18.81	19.57	0.76	0.10	0.60	1.37	1.59	-22.8	30.9	1.29	0.450	
23 22 14.747	-10 37 24.06	*	17.08	17.36	0.28	0.09	1.11	1.10	0.96	-26.2	31.1	0.21	0.750	X
23 23 55.455	+00 35 50.26	*	18.28	18.74	0.46	0.11	0.30	15.70	16.22	-27.5	33.2	1.79	2.290	
23 24 48.319	+00 36 35.51	*	18.33	19.11	0.79	0.09	1.14	34.72	98.73	-25.4	33.4	2.82	1.126	
23 27 34.797	+00 22 32.63	*	18.63	19.43	0.79	0.11	1.72	38.11	76.66	-25.8	33.6	2.80	1.490	CJ
23 30 34.453	-02 15 00.26	*	16.91	17.78	0.87	0.13	0.17	18.04	19.14	-26.0	32.4	1.61	0.810	
23 30 54.417	-01 20 53.24	*	18.68	19.20	0.52	0.12	0.39	6.77	7.44	-27.6	33.1	1.60	2.904	
23 31 32.836	+01 06 20.94	*	18.24	19.23	0.98	0.12	0.40	42.40	41.96	-27.3	33.8	2.38	2.614	
23 32 25.585	-09 57 56.42	*	18.83	19.60	0.77	0.07	0.29	1270.43	1449.58	-25.9	34.9	4.13	1.680	
23 33 04.077	-10 44 27.74	gR	18.75	19.53	0.78	0.07	0.21	1.28	1.84	-22.6	30.8	1.34	0.410	
23 33 16.697	-01 31 07.47	*	18.78	19.39	0.62	0.10	0.04	173.20	181.56	-25.0	33.7	3.20	1.060	o,X
23 34 19.700	-01 28 25.10	*	17.49	18.05	0.55	0.11	0.25	3.26	2.91	-25.6	31.7	0.95	0.790	
23 34 41.871	-02 15 15.08	*	17.52	18.71	1.19	0.12	0.36	1.63	1.43	-26.2	31.8	0.86	1.327	
23 34 46.396	-09 08 12.35	*	17.86	18.66	0.80	0.08	0.28	25.48	26.85	-28.5	33.8	1.92	3.300	dmpLα
23 35 20.432	-01 31 09.81	*	17.97	18.67	0.71	0.11	0.52	662.33	726.21	-26.0	34.4	3.50	1.188	o
23 35 31.876	-09 57 49.23	*	18.46	18.25	-0.21	0.07	0.17	3.52	3.61	-25.7	31.8	1.06	0.900	
23 35 34.682	-09 27 39.34	*	18.68	18.30	-0.38	0.07	0.10	11.48	11.55	-27.4	32.9	1.50	1.810	
23 36 11.627	-09 54 27.05	*	18.73	18.54	-0.19	0.08	0.19	1.83	1.60	-27.1	32.1	0.80	1.760	HiBAL
23 36 24.061	+00 02 46.32	*	17.04	17.89	0.86	0.09	0.37	16.63	17.07	-26.6	32.7	1.57	1.100	
23 38 14.732	-01 40 08.54	*	18.71	19.29	0.58	0.09	0.14	1.90	1.34	-25.1	31.7	1.18	1.060	
23 38 18.267	-00 56 10.58	*	18.24	19.14	0.90	0.09	0.05	12.16	12.27	-24.8	32.3	1.95	0.896	
23 38 33.990	-09 00 38.95	*	17.62	17.65	0.03	0.07	0.37	1.71	1.78	-24.3	30.8	0.58	0.375	
23 38 38.227	-00 35 13.51	*	18.45	18.77	0.32	0.08	0.52	4.61	5.42	-27.8	32.9	1.30	2.670	
23 39 30.027	+00 30 17.45	*	18.07	18.61	0.54	0.10	0.28	26.43	27.43	-28.3	33.7	1.92	3.040	
23 40 23.671	-00 53 27.08	*	16.93	17.38	0.45	0.09	0.20	115.55	116.90	-28.6	34.0	2.12	2.090	
23 42 12.855	+01 10 02.13	*	18.47	18.93	0.46	0.08	0.47	4.37	5.35	-25.5	32.1	1.49	1.070	
23 42 53.599	+01 15 21.48	*	18.70	19.27	0.57	0.08	0.36	3.41	3.54	-27.0	32.6	1.34	2.320	o
23 44 03.119	+00 38 03.90	*	16.75	17.07	0.33	0.07	0.17	1.57	1.65	-27.7	31.7	0.22	1.230	
23 44 40.035	-00 32 31.65	*	17.33	17.49	0.16	0.09	0.34	16.82	18.32	-25.1	32.0	1.51	0.500	
23 45 40.413	-09 36 10.28	*	18.60	18.41	-0.19	0.09	0.79	7.34	9.52	-26.4	32.5	1.51	1.270	
23 47 11.497	-10 37 42.18	*	17.45	17.64	0.20	0.09	0.58	1.08	1.41	-28.0	32.0	0.33	1.780	LoBAL
23 48 30.419	+00 39 18.63	*	17.65	17.79	0.14	0.07	0.09	2.86	3.74	-28.1	32.5	0.79	2.000	o
23 48 36.040	-01 46 30.53	*	18.78	19.62	0.85	0.08	0.78	1.95	1.40	-25.4	31.9	1.29	1.390	
23 49 03.610	-09 51 09.13	*	18.28	18.39	0.10	0.08	0.42	1.75	1.77	-25.8	31.6	0.80	0.990	
23 49 14.884	-01 27 17.63	*	17.99	18.54	0.55	0.09	0.50	27.69	27.93	-27.7	33.5	1.95	2.310	
23 49 21.895	-11 13 52.30	*	18.81	18.26	-0.54	0.08	0.40	5.91	6.67	-27.9	32.8	1.22	2.230	
23 50 08.225	-10 17 35.69	*	18.57	18.91	0.34	0.09	0.80	55.81	62.96	-26.0	33.4	2.52	1.310	
23 50 13.010	-02 06 14.27	*	18.57	19.00	0.43	0.09	0.23	45.29	46.41	-26.5	33.4	2.40	1.675	
23 53 06.491	-09 25 48.29	gR	18.04	19.79	1.75	0.10	0.28	3.63	2.93	-21.6	30.8	1.76	0.290	
23 53 14.273	-10 41 06.02	gR	17.24	17.94	0.70	0.11	0.25	9.83	10.10	-26.8	32.5	1.35	1.240	
23 53 21.050	-08 59 30.83	*	18.25	18.63	0.38	0.10	0.40	16.98	18.86	-26.8	33.0	1.86	1.650	
23 54 09.167	-00 19 47.67	*	17.09	18.11	1.02	0.08	0.39	344.79	346.10	-24.3	33.2	3.05	0.460	o,No spec
23 55 20.603	+00 07 47.56	*	17.64	18.42	0.78	0.11	0.06	17.72	18.92	-26.0	32.7	1.83	1.070	o
23 57 37.982	+00 32 28.34	*	18.38	19.18	0.80	0.09	0.41	1.32	3.28	-24.9	31.8	1.38	0.952	
23 58 10.875	-10 20 08.98	*	17.94	19.28	1.34	0.09	0.54	758.05	770.09	-26.1	34.6	3.73	1.630	o
23 59 30.722	+01 19 58.69	*	18.04	18.81	0.77	0.08	0.82	1.58	2.59	-23.9	31.2	1.19	0.520	
00 00 01.245	-02 02 00.18	*	18.31	19.64	1.33	0.10	0.61	1.25	1.45	-25.3	31.8	1.18	1.356	
00 00 17.372	-08 51 23.27	*	18.26	18.93	0.67	0.10	0.49	9.41	9.77	-25.8	32.5	1.73	1.250	
00 00 50.609	-10 21 56.00	*	18.03	18.53	0.51	0.11	0.09	20.01	20.39	-28.0	33.5	1.79	2.630	
00 02 21.139	+00 21 49.48	*	17.97	18.63	0.66	0.08	0.21	12.86	13.88	-28.3	33.4	1.63	3.058	
00 02 22.488	-00 04 43.40	*	17.47	18.18	0.71	0.09	0.08	4.23	3.89	-25.6	31.8	1.11	0.810	o
00 04 42.191	+00 00 23.02	*	18.07	18.81	0.74	0.10	0.34	4.10	3.71	-25.4	32.0	1.33	1.007	
00 05 07.090	-10 10 08.55	*	18.33	19.26	0.93	0.10	0.37	82.33	94.62	-25.6	33.5	2.84	1.300	
00 05 07.065	-01 32 45.33	gR	17.65	18.32	0.67	0.09	0.31	62.26	63.87	-27.2	33.6	2.26	1.710	o
00 06 22.611	-00 04 24.48	*	18.57	19.45	0.88	0.14	0.30	3111.27	3879.24	-24.9	35.0	4.56	1.037	o,No spec
00 07 10.004	+00 53 28.51	gR	16.46	17.51	1.05	0.09	0.55	1.55	1.44	-24.0	30.5	0.48	0.317	o,X
00 10 02.998	-01 01 06.60	*	17.83	18.52	0.69	0.09	0.66	1.29	1.72	-24.3	31.1	0.89	0.554	
00 11 04.666	+01 22 55.79	*	17.40	18.25	0.85	0.07	0.42	3.63	4.92	-26.3	32.1	1.17	1.119	
00 12 14.201	-09 59 22.94	*	18.31	19.55	1.24	0.10	0.32	3.03	3.18	-25.2	32.0	1.49	1.260	o
00 12 14.805	-01 31 28.64	gB	16.68	17.33	0.65	0.10	0.09	1.61	1.08	-27.1	31.6	0.32	1.070	o
00 12 24.033	-10 22 26.63	gR	16.04	16.97	0.93	0.11	0.45	3.88	3.73	-23.8	30.7	0.67	0.228	
00 14 20.369	-09 18 49.36	*	16.89	17.62	0.74	0.11	0.09	5.73	4.74	-26.8	32.2	0.99	1.090	
00 14 28.757	+00 39 04.94	*	18.35	19.88	1.53	0.07	0.56	4.45	4.05	-24.7	32.1	1.78	1.160	
00 14 38.279	-01 07 50.31	*	18.28	19.95	1.66	0.12	0.23	1.41	1.59	-25.7	32.0	1.30	1.800	LoBAL?
00 14 44.078	-00 00 17.99	*	17.22	18.62	1.40	0.07	0.84	1.45	1.51	-26.7	31.9	0.77	1.560	o,No spec
00 15 07.023	-00 08 00.92	*	17.59	19.12	1.53	0.07	0.19	12.67	13.53	-26.4	32.9	1.91	1.700	o,X

TABLE 1—*Continued*

RA (1)	Dec (2)	Cl (3)	R (4)	B (5)	B-R (6)	A(R) (7)	Sep (8)	S_p (9)	S_i (10)	M_B (11)	$\log L_R$ (12)	$\log R^*$ (13)	z (14)	Notes (15)
00 19 12.613	-08 39 46.50	*	16.58	17.09	0.51	0.11	0.20	1.38	1.12	-25.8	31.0	0.22	0.580	
00 22 44.296	-01 45 51.07	*	17.23	18.71	1.48	0.13	0.13	8.31	9.48	-24.6	32.0	1.69	0.690	o,No spec
00 22 49.208	-10 39 55.44	*	17.33	17.88	0.55	0.09	0.80	2.03	1.88	-24.3	30.9	0.73	0.414	
00 24 11.651	-00 43 49.17	*	17.31	18.60	1.29	0.06	0.96	1.17	0.99	-25.0	31.2	0.73	0.770	o,No spec
00 27 17.354	+00 37 23.77	*	17.11	18.37	1.26	0.06	0.52	3.50	3.73	-26.4	32.1	1.09	1.230	o,No spec
00 27 56.208	-08 37 18.17	*	18.46	19.11	0.66	0.10	0.28	2.98	2.53	-25.3	31.9	1.31	1.060	
00 31 11.277	-00 11 21.63	*	18.49	19.87	1.37	0.06	0.77	1.30	1.83	-25.4	32.0	1.35	1.510	
00 31 36.487	-01 36 22.04	*	18.23	19.11	0.88	0.07	0.37	13.54	14.06	-27.2	33.2	1.87	2.380	o
00 34 19.186	+01 18 35.82	*	18.50	18.56	0.07	0.06	0.40	2.33	1.46	-25.3	31.6	1.00	0.870	
00 34 38.351	-01 43 08.62	*	18.42	18.65	0.23	0.07	1.15	69.88	111.82	-25.4	33.3	2.71	0.940	
00 34 43.936	-00 54 13.04	*	18.18	19.07	0.89	0.06	0.28	67.42	70.15	-24.2	32.8	2.71	0.656	
00 35 52.963	-09 11 50.59	*	18.80	20.14	1.34	0.10	0.58	90.87	97.00	-24.1	33.3	3.24	1.000	
00 36 06.856	-09 32 30.01	gR	18.08	19.15	1.07	0.09	0.64	71.61	96.23	-25.5	33.5	2.82	1.180	
00 36 11.290	-10 37 37.09	*	18.31	19.01	0.69	0.07	0.85	1.32	0.79	-26.5	31.9	0.85	1.670	
00 39 31.593	-11 11 02.84	gR	18.37	20.04	1.67	0.08	0.35	273.42	295.94	-22.8	33.3	3.74	0.556	
00 40 57.606	-01 46 32.00	*	18.12	18.80	0.69	0.06	0.15	593.72	616.31	-25.8	34.3	3.49	1.175	o
00 41 25.968	-01 43 24.43	*	16.95	16.81	-0.14	0.06	8.53	272.43	466.78	-28.7	34.4	2.52	1.670	DBL
00 41 49.026	-11 08 54.99	*	18.62	19.48	0.86	0.08	0.68	1.12	0.63	-25.2	31.5	1.02	1.200	
00 43 22.368	-00 13 43.95	*	18.35	19.11	0.75	0.05	0.11	6.93	6.80	-26.2	32.6	1.62	1.590	
00 43 32.708	+00 24 59.93	*	18.90	19.49	0.58	0.05	0.14	108.53	111.57	-25.0	33.5	3.02	1.127	o,No spec
00 44 13.525	+00 52 01.34	*	17.91	18.49	0.59	0.06	20.37	1.64	3.24	-25.6	31.8	1.11	0.940	DBL
00 44 18.948	-09 00 09.68	*	18.75	19.28	0.53	0.09	0.31	4.08	3.46	-24.9	31.9	1.52	0.965	
00 44 43.650	-09 46 24.81	*	18.84	19.56	0.72	0.10	0.52	1.56	1.75	-26.5	32.2	1.17	2.100	
00 46 13.548	+01 04 25.78	*	17.74	18.06	0.31	0.06	0.08	3.04	2.92	-28.0	32.5	0.80	2.150	o,HiBAL
00 47 08.565	-09 32 09.92	gR	18.82	20.10	1.28	0.09	1.05	195.06	203.51	-26.5	34.5	3.41	2.620	
00 48 06.084	-01 03 22.14	*	17.71	18.24	0.53	0.08	0.59	1.61	2.27	-28.2	32.5	0.72	2.530	o
00 50 26.772	+00 31 57.30	*	18.32	18.87	0.55	0.06	0.42	64.34	66.92	-25.8	33.3	2.54	1.210	
00 51 15.102	-09 02 09.13	*	18.58	19.98	1.41	0.10	0.28	1.42	0.83	-24.8	31.7	1.31	1.260	
00 51 30.488	+00 41 49.91	*	17.66	18.15	0.49	0.07	0.15	13.70	13.78	-26.5	32.6	1.57	1.190	o
00 51 56.903	+01 26 12.91	*	18.25	18.85	0.60	0.07	1.04	22.64	29.91	-26.0	33.0	2.18	1.290	
00 52 05.568	+00 35 38.25	*	15.73	16.61	0.87	0.06	0.32	81.46	87.95	-25.5	32.5	1.86	0.400	o,X
00 55 50.704	-10 19 06.19	*	18.68	18.90	0.22	0.10	0.67	2.07	3.03	-22.6	30.8	1.32	0.310	
00 57 29.073	-09 32 58.73	*	18.14	18.13	-0.01	0.11	0.66	1.90	1.78	-24.7	31.1	0.78	0.556	
00 59 05.511	+00 06 51.70	*	17.47	17.85	0.39	0.07	0.33	2324.98	2415.95	-25.6	34.4	3.75	0.720	o,X
01 00 33.512	+00 22 00.16	*	17.32	17.97	0.65	0.08	0.23	18.67	18.90	-25.6	32.4	1.69	0.750	
01 00 39.857	-01 31 27.19	gR	17.95	19.72	1.77	0.13	0.17	39.22	41.20	-27.7	34.0	2.51	3.642	
01 02 05.607	-01 50 38.87	*	17.38	18.21	0.83	0.10	0.53	2.37	1.81	-26.7	32.0	0.82	1.320	o
01 02 05.969	+00 11 56.76	*	16.79	17.44	0.65	0.09	1.01	56.32	67.35	-26.0	32.9	2.03	0.725	
01 02 49.663	-08 53 44.31	*	18.00	18.50	0.50	0.10	0.29	8.35	9.05	-27.0	32.7	1.49	1.680	
01 03 21.783	-00 24 01.23	*	18.47	19.11	0.64	0.10	0.28	3.67	3.15	-25.8	32.1	1.37	1.325	
01 03 28.728	-11 04 14.60	*	18.33	18.39	0.06	0.08	0.19	47.53	50.17	-27.7	33.7	2.15	2.190	
01 03 52.474	+00 37 39.74	*	16.81	17.82	1.02	0.09	0.07	2.39	2.22	-25.6	31.4	0.74	0.700	
01 06 44.125	-10 34 10.56	*	17.92	17.66	-0.26	0.09	0.50	128.37	265.77	-24.8	33.1	2.75	0.470	X
01 08 26.839	-00 37 24.12	*	17.49	18.18	0.69	0.09	0.21	883.60	903.38	-26.8	34.6	3.38	1.380	o
01 09 05.906	-09 28 49.05	*	18.80	18.95	0.15	0.13	1.04	1.50	1.32	-27.6	32.3	0.82	2.570	
01 10 13.400	-02 20 06.80	*	17.29	18.32	1.03	0.11	14.73	20.19	41.09	-25.8	32.9	2.14	0.960	o,DBL
01 11 29.900	+00 34 31.50	*	18.74	19.75	1.01	0.08	0.89	21.98	34.80	-25.2	33.1	2.60	1.320	
01 13 08.620	-08 52 37.08	gB	18.55	19.48	0.93	0.13	0.20	2.60	3.20	-24.1	31.6	1.52	0.760	
01 13 12.106	-10 14 21.58	*	18.72	19.38	0.67	0.09	0.27	519.08	524.76	-25.5	34.3	3.63	1.320	
01 15 17.110	-01 27 04.52	*	17.37	17.65	0.29	0.18	0.16	1025.07	1107.52	-27.3	34.7	3.26	1.370	o,X
01 18 34.631	-08 54 39.74	*	18.48	19.88	1.40	0.09	0.53	137.48	163.67	-25.0	33.8	3.33	1.320	
01 19 10.015	+01 31 28.25	*	17.43	17.94	0.51	0.07	0.50	2.45	2.15	-24.7	31.2	0.82	0.520	
01 20 44.819	-02 16 17.14	*	18.36	18.93	0.57	0.11	0.59	1.39	1.94	-26.1	31.9	1.01	1.393	
01 22 40.125	-00 32 39.56	*	18.04	18.23	0.20	0.12	0.17	1.09	0.75	-25.7	31.3	0.54	0.883	
01 22 48.071	-09 35 46.92	gR	18.38	18.27	-0.10	0.10	0.33	23.82	26.49	-25.4	32.6	1.95	0.780	
01 25 17.191	-00 18 29.90	*	18.60	18.13	-0.47	0.07	1.14	334.34	538.09	-28.1	34.8	3.07	2.270	o
01 25 28.853	-00 05 56.20	*	16.37	16.58	0.20	0.09	0.08	1481.35	1524.09	-27.8	34.6	3.00	1.070	o,X
01 27 02.534	+01 14 13.80	*	17.60	19.31	1.71	0.08	0.80	1.06	1.14	-25.3	31.5	0.96	1.160	
01 28 27.474	-10 32 50.69	gR	17.70	18.55	0.85	0.09	0.87	1.14	1.24	-23.0	30.4	0.80	0.312	
01 28 41.876	-00 33 16.79	*	18.34	19.25	0.91	0.08	0.17	3.03	2.96	-26.2	32.2	1.31	1.650	HiBAL
01 29 05.332	-00 54 50.42	*	18.49	18.64	0.15	0.08	0.18	11.09	11.19	-24.8	32.1	1.73	0.710	
01 29 12.494	-08 29 25.29	*	17.96	18.13	0.17	0.06	0.71	3.53	5.38	-25.7	31.9	1.20	0.830	
01 29 44.459	-09 14 16.07	*	18.24	18.66	0.42	0.08	0.48	6.19	6.16	-24.7	31.8	1.49	0.700	
01 30 08.910	-10 19 07.33	*	17.84	18.07	0.22	0.11	0.53	53.86	70.49	-26.2	33.2	2.27	1.000	
01 30 43.001	-01 35 08.24	*	18.82	19.87	1.05	0.11	1.09	1.47	1.52	-24.7	31.7	1.31	1.160	
01 30 50.967	-10 46 30.74	*	17.41	17.66	0.25	0.12	0.37	86.31	92.12	-27.8	33.7	2.16	1.640	
01 31 46.436	-08 41 04.14	*	18.47	19.48	1.01	0.07	0.27	5.47	5.35	-26.0	32.5	1.66	1.650	
01 32 49.395	+00 26 27.00	*	18.64	19.25	0.60	0.07	0.44	3.51	3.37	-27.8	32.8	1.28	3.170	
01 34 27.294	-01 33 50.16	*	17.77	18.47	0.70	0.10	0.19	9.57	9.59	-25.2	32.1	1.59	0.780	
01 35 15.239	-02 13 49.26	*	17.12	17.71	0.60	0.10	0.03	22.42	22.81	-28.0	33.2	1.56	1.820	HiBAL
01 35 17.531	-00 19 39.46	gR	17.55	18.60	1.05	0.09	0.27	1.57	1.51	-22.9	30.5	0.92	0.312	
01 37 25.135	-00 49 06.58	*	18.48	19.30	0.81	0.08	0.21	2.50	2.50	-25.4	31.9	1.29	1.200	
01 37 45.645	-02 11 09.34	*	18.50	19.14	0.64	0.11	0.12	4.18	5.31	-26.3	32.5	1.51	1.660	
01 38 08.093	-01 45 18.79	*	18.66	19.87	1.21	0.09	5.96	178.96	248.49	-23.3	33.4	3.58	0.640	DBL
01 39 42.009	-01 37 46.35	*	18.61	19.29	0.69	0.09	0.40	1.80	2.23	-25.8	32.0	1.22	1.440	
01 40 00.259	-01 12 00.35	*	18.50	18.63	0.13	0.08	0.24	2.61	3.25	-25.0	31.6	1.18	0.780	
01 40 18.199	-01 38 05.94	*	17.64	17.97	0.34	0.08	0.02	1.51	0.95	-28.2	32.2	0.46	2.240	o,HiBAL
01 41 23.047	-00 24 22.03	*	18.18	18.70	0.52	0.08	0.27	8.49	8.01	-27.9	33.1	1.47	2.610	
01 45 52.531	+00 51 50.66	*	18.55	19.37	0.82	0.07	0.91	1.08	0.96	-24.6	31.3	0.99	0.910	
01 46 09.846	+00 43 20.98	*	18.20	19.14	0.95	0.08	0.20	13.49	13.27	-24.8	32.4	1.99	0.890	

TABLE 1—*Continued*

RA (1)	Dec (2)	Cl (3)	R (4)	B (5)	B-R (6)	A(R) (7)	Sep (8)	S_p (9)	S_i (10)	M_B (11)	$\log L_R$ (12)	$\log R^*$ (13)	z (14)	Notes (15)
01 48 12.829	-00 51 09.01	*	18.41	19.18	0.77	0.10	0.32	3.19	3.43	-26.5	32.4	1.32	1.820	HiBAL
01 49 40.118	+00 17 18.50	*	18.06	18.61	0.54	0.11	0.33	1.64	1.50	-26.5	31.9	0.81	1.430	
01 51 05.846	-00 34 26.01	*	18.65	19.69	1.04	0.08	0.38	1.76	4.15	-22.0	31.0	1.78	0.335	X
01 51 06.692	-09 32 00.45	*	18.17	18.91	0.74	0.06	0.09	43.80	44.66	-27.9	33.9	2.26	2.850	o
01 51 22.083	-08 19 29.32	*	18.67	19.48	0.81	0.07	0.71	5.08	8.82	-24.3	32.1	1.95	0.820	
01 51 50.658	-01 12 19.01	*	18.52	18.74	0.22	0.08	0.36	3.00	3.16	-25.0	31.7	1.21	0.810	
01 51 53.304	-00 28 50.27	*	17.52	18.49	0.97	0.08	0.15	12.14	12.28	-27.4	33.0	1.59	1.990	
01 52 37.079	-01 43 58.60	gB	15.77	16.74	0.97	0.08	0.21	1.57	1.52	-27.1	31.4	0.10	0.850	
01 52 59.111	-01 29 40.77	*	18.22	18.61	0.39	0.08	0.47	35.97	38.33	-27.3	33.5	2.13	2.010	o
01 53 45.346	-10 08 40.06	*	18.86	19.33	0.46	0.06	0.30	3.95	4.13	-26.5	32.5	1.46	1.900	HiBAL
01 54 53.054	-09 55 35.12	*	17.47	18.65	1.19	0.06	0.13	1.75	1.69	-26.2	31.8	0.87	1.280	
01 55 09.014	+01 15 23.08	*	18.02	18.55	0.53	0.08	0.34	88.38	91.14	-26.7	33.7	2.52	1.540	
01 55 45.772	-08 11 18.46	*	18.69	19.84	1.15	0.06	0.10	7.22	7.70	-25.4	32.6	1.96	1.530	
01 58 43.810	-08 59 41.39	*	18.70	19.34	0.64	0.06	0.18	6.72	7.04	-25.5	32.4	1.74	1.310	
01 59 42.451	-08 08 17.37	*	18.43	19.45	1.02	0.07	0.66	1.12	0.82	-25.1	31.5	1.01	1.130	
02 00 03.957	+01 25 12.44	*	18.03	18.56	0.53	0.07	0.26	537.75	645.93	-26.0	34.3	3.41	1.160	o
02 00 21.301	-03 37 25.01	*	18.87	19.21	0.33	0.07	0.38	4.53	4.41	-24.6	31.9	1.55	0.850	
02 00 22.031	-08 45 11.76	*	18.58	19.63	1.04	0.07	0.44	7.75	7.34	-26.2	32.8	1.85	1.930	HiBAL
02 00 56.464	-05 34 56.02	*	18.38	18.82	0.43	0.07	0.04	3.03	2.43	-25.2	31.7	1.21	0.900	
02 02 27.319	-01 45 23.05	*	18.02	18.99	0.98	0.07	0.32	25.13	30.77	-25.5	32.9	2.27	1.118	
02 02 39.912	-03 02 07.96	*	18.86	18.64	-0.22	0.07	0.18	118.45	122.18	-26.3	33.7	2.70	1.350	
02 03 24.131	-07 09 40.79	*	18.83	19.29	0.46	0.06	0.14	7.15	7.68	-25.2	32.3	1.78	1.120	
02 03 50.879	-02 06 50.87	*	18.03	19.30	1.27	0.08	0.43	2.28	2.49	-24.8	31.7	1.31	0.960	
02 04 28.554	-07 02 22.87	*	18.00	18.73	0.73	0.06	1.33	4.06	5.80	-26.5	32.4	1.40	1.480	CJ
02 04 46.605	-07 21 10.80	*	18.56	19.14	0.57	0.05	0.31	55.74	60.29	-26.3	33.5	2.57	1.650	
02 04 48.310	-09 44 09.43	*	18.45	19.41	0.96	0.06	0.49	3.07	2.78	-24.8	31.8	1.45	1.000	
02 06 36.638	-03 17 40.57	*	17.61	18.45	0.84	0.06	0.68	1.46	1.01	-26.2	31.6	0.72	1.180	
02 07 14.362	+01 18 07.01	*	17.98	18.92	0.94	0.07	0.33	3.74	12.74	-25.2	32.4	1.87	0.970	
02 08 03.007	-05 02 59.31	*	18.47	18.75	0.28	0.06	0.87	1.10	0.85	-27.0	31.9	0.66	1.850	
02 09 30.760	-04 38 26.79	*	16.62	17.04	0.42	0.06	0.57	201.45	225.43	-27.5	33.8	2.35	1.130	
02 10 08.503	+01 18 40.31	*	17.88	18.52	0.64	0.07	0.40	6.60	6.54	-25.4	32.0	1.44	0.870	
02 10 28.263	-10 15 38.95	*	17.84	18.75	0.91	0.07	0.86	2.68	2.60	-25.9	31.9	1.10	1.210	
02 10 39.907	-01 52 13.40	*	17.10	17.68	0.58	0.08	0.46	1.51	1.76	-28.6	32.3	0.40	2.370	
02 12 25.600	+01 00 56.08	*	18.74	18.55	-0.20	0.09	0.59	18.34	51.08	-24.1	32.5	2.38	0.510	X
02 12 29.850	+00 09 33.87	*	18.54	19.94	1.41	0.09	0.51	1.14	0.79	-23.0	30.9	1.28	0.580	
02 12 59.610	-00 30 29.88	gR	17.59	18.05	0.46	0.09	0.69	1.25	1.26	-24.0	30.6	0.59	0.390	
02 13 09.329	-00 47 35.13	*	18.01	18.58	0.58	0.08	0.08	11.11	10.78	-26.6	32.7	1.62	1.510	
02 13 29.881	-05 21 39.28	*	17.91	18.91	1.00	0.06	0.13	2.32	2.96	-24.6	31.6	1.26	0.750	
02 15 07.596	-07 02 08.72	*	17.82	18.81	0.99	0.07	0.24	102.52	167.59	-27.4	34.2	2.84	2.220	
02 16 12.209	-01 05 18.75	*	17.41	17.82	0.41	0.09	0.08	148.05	152.65	-27.4	33.9	2.46	1.480	o,new z
02 16 40.746	-04 44 05.08	*	15.88	16.91	1.02	0.05	0.18	90.60	93.64	-27.0	33.2	1.94	0.870	
02 18 00.144	-06 05 49.81	*	18.68	19.67	0.99	0.07	0.45	21.78	21.98	-25.2	32.9	2.37	1.290	
02 19 49.130	-07 37 48.97	*	18.73	19.73	0.99	0.06	0.15	6.89	7.23	-25.2	32.4	1.91	1.320	
02 20 02.346	-01 43 52.67	gR	18.58	19.76	1.18	0.07	0.87	42.36	46.20	-22.7	32.4	2.83	0.470	
02 20 27.564	+01 14 02.02	*	17.85	18.43	0.57	0.10	0.06	6.21	6.22	-26.5	32.4	1.33	1.330	
02 21 00.743	-01 22 12.16	*	18.26	19.18	0.92	0.09	0.54	1.80	1.57	-25.5	31.8	1.10	1.210	LoBAL
02 21 13.157	+01 01 03.33	gR	18.08	19.19	1.11	0.10	0.14	26.73	29.74	-22.6	31.9	2.43	0.354	
02 25 08.085	+00 17 07.32	*	18.55	19.23	0.68	0.11	0.08	274.34	277.72	-23.5	33.2	3.39	0.523	o
02 28 27.900	-01 10 46.21	*	18.83	19.26	0.43	0.09	0.36	2.60	3.03	-25.3	31.9	1.36	1.130	o,No spec
02 30 16.829	-00 07 43.88	*	17.84	18.10	0.26	0.06	0.94	1.95	2.83	-25.8	31.7	0.90	0.877	
02 32 34.281	-09 10 52.76	*	18.46	19.34	0.87	0.08	0.48	1.21	1.18	-24.5	31.3	1.03	0.850	
02 33 13.810	-00 12 15.26	*	18.11	19.18	1.07	0.06	0.10	3.95	5.69	-24.5	31.9	1.64	0.810	
02 36 15.078	-01 21 32.53	*	17.66	18.31	0.66	0.08	0.04	4.88	4.44	-26.1	32.1	1.20	1.090	
02 38 01.922	-08 31 22.69	*	18.12	18.70	0.58	0.07	0.09	9.23	9.75	-25.3	32.2	1.67	0.900	
02 38 22.472	+01 23 53.75	*	17.97	18.83	0.86	0.08	0.40	22.15	21.93	-26.3	33.0	2.03	1.433	
02 38 59.230	-00 01 58.11	*	17.35	18.24	0.89	0.08	0.71	1.00	1.03	-25.5	31.2	0.52	0.811	
02 39 14.009	-01 18 11.52	*	18.40	18.52	0.12	0.08	7.52	115.33	136.72	-27.1	34.0	2.66	1.780	DBL
02 39 45.961	-07 09 45.40	*	18.71	19.13	0.42	0.06	0.16	6.13	6.54	-24.9	32.1	1.67	0.930	
02 42 40.314	+00 57 27.63	gR	16.22	16.57	0.35	0.09	0.21	3.57	3.58	-26.3	31.4	0.43	0.570	o,X
02 42 47.672	-01 57 49.58	*	18.66	19.23	0.58	0.08	0.27	184.75	215.36	-23.8	33.3	3.27	0.610	o
02 45 34.032	+01 08 13.76	*	18.64	20.31	1.67	0.11	0.62	6.06	11.67	-24.9	32.8	2.33	1.530	o
02 46 46.896	-01 45 34.08	*	17.14	18.43	1.28	0.13	4.11	26.78	49.45	-27.2	33.5	2.19	1.780	DBL
02 47 06.662	+00 23 18.79	gB	17.32	18.87	1.56	0.10	0.25	1.80	1.66	-23.0	30.7	1.08	0.364	
02 49 40.220	-08 34 26.37	*	18.12	18.23	0.11	0.08	0.20	46.46	46.85	-26.4	33.2	2.13	1.200	
02 50 03.320	-08 52 16.20	*	18.35	18.76	0.41	0.08	0.22	6.75	7.12	-27.2	32.8	1.46	2.060	
02 50 48.691	+00 02 08.05	*	18.43	18.65	0.22	0.20	0.67	12.66	19.87	-25.0	32.4	1.98	0.770	o
02 51 56.300	+00 57 06.90	*	17.81	18.23	0.42	0.19	0.33	7.63	8.14	-24.2	31.6	1.46	0.470	o
02 53 40.950	+00 11 10.40	*	18.12	18.81	0.69	0.21	0.49	7.50	7.64	-26.7	32.7	1.54	1.680	o,No spec
02 56 14.046	+00 39 40.98	*	18.80	19.19	0.39	0.23	0.32	11.55	12.58	-24.8	32.4	1.98	0.920	o
02 56 25.641	-01 19 11.51	*	18.41	18.70	0.29	0.17	0.35	25.78	27.56	-27.7	33.5	1.99	2.490	HiBAL
02 58 38.089	-01 54 11.21	gR	17.98	18.14	0.16	0.23	0.29	1.05	1.14	-24.0	30.6	0.58	0.410	o,No spec
02 59 28.511	-00 19 59.84	*	17.21	17.46	0.25	0.29	0.32	225.85	224.97	-28.5	34.3	2.44	2.000	o
02 59 37.445	+00 37 35.96	*	15.87	16.56	0.69	0.25	0.94	1.10	0.78	-26.2	30.8	-0.08	0.530	o
03 01 40.991	+01 15 51.10	*	18.75	19.27	0.53	0.26	0.48	3.15	2.85	-26.3	32.3	1.33	1.770	o
03 11 29.317	+00 56 38.92	*	18.84	18.67	-0.17	0.33	0.47	3.13	3.72	-26.5	32.3	1.18	1.500	
03 12 26.182	-00 37 08.97	*	18.72	17.71	-1.01	0.20	0.61	20.45	24.02	-25.4	32.3	1.70	0.621	
03 13 18.648	+00 36 24.18	*	17.86	17.51	-0.34	0.24	0.59	11.13	13.52	-27.3	32.7	1.30	1.250	
03 14 30.035	+01 17 36.16	*	18.54	18.23	-0.31	0.36	0.51	18.04	18.75	-26.5	32.8	1.74	1.210	
03 15 42.470	-01 51 22.55	*	16.81	16.74	-0.08	0.23	0.67	97.26	120.95	-28.4	33.8	1.92	1.480	o
03 16 31.392	+01 37 29.77	*	17.98	17.69	-0.29	0.32	0.35	5.73	4.75	-26.4	32.1	1.03	0.950	o

Table 1—*Continued*

RA (1)	Dec (2)	Cl (3)	R (4)	B (5)	B-R (6)	A(R) (7)	Sep (8)	S_p (9)	S_i (10)	M_B (11)	$\log L_R$ (12)	$\log R^*$ (13)	z (14)	Notes (15)
03 20 28.385	-01 26 36.55	*	17.30	16.72	-0.58	0.21	0.03	3.95	3.60	-25.7	31.3	0.54	0.460	

Note. — Descriptions of table columns:
Cols 1–2: FIRST radio positions (J2000).
Col 3: Optical morphology in the APM catalog. *: stellar on both plates, gR: nonstellar on R plate, gB: nonstellar on B plate.
Cols 4–6: Extinction-corrected APM magnitudes and color. Note that magnitudes are unreliable for objects brighter than ∼ 15th magnitude (Paper II).
Col 7: Extinction correction (magnitudes) that was applied to R, computed as $2.7\,E(B-V)$ using the extinction maps of Schlegel et al. (1998). The correction for B is $4.3\,E(B-V) = 1.59\,A(R)$.
Col 8: Separation between radio and optical positions (arcsec.)
Cols 9-10: 20 cm peak (col. 9) and integrated (col. 10) flux densities in mJy from the FIRST catalog.
Col 11: Absolute B magnitude.
Col 12: Log of radio luminosity (erg cm^{-2} s^{-1} Hz^{-1}) at a rest-frame frequency of 5 GHz, assuming spectral index $\alpha = -0.5$ ($F_\nu \propto \nu^\alpha$).
Col 13: K-corrected 5 GHz radio to 2500 Å optical luminosity ratio using the definition of Stocke et al. (1992).
Col 14: Redshift.
Col 15: Notes on individual objects. *o*: Previously known QSO from NASA Extragalactic Database (NED) or from Véron-Cetty & Véron (1998) catalog. *new z*: Newly determined redshift for previously known object. *No spec*: A previously known quasar for which no spectrum appears in Fig. 9. *DBL*: Object included in sample as central-component of core-less double. *CJ*: Object included in sample as match to core-jet source. *X*: X-ray source in ROSAT BSC (Voges et al. 1996). *I*: Infrared source in IRAS FSC (Moshir et al. 1992). *HiBAL, LoBAL, FeLoBAL*: Object shows broad absorption lines from high-ionization, low-ionization, or iron + low-ionization elements. If followed by *?*, the object fails the "balnicity" test (Weymann et al. 1991) but may nonetheless be a BAL. *dmpLα*: Object shows damped Lyα absorption. *?*: Quasar classification is considered uncertain.

Table 2

Narrow-line AGN in FBQS Candidate List

RA (1)	Dec (2)	Cl (3)	R (4)	B (5)	B-R (6)	A(R) (7)	Sep (8)	S_p (9)	S_i (10)	M_B (11)	$\log L_R$ (12)	$\log R^*$ (13)	z (14)	Notes (15)
21 17 05.992	-06 40 46.07	gR	17.91	19.51	1.60	0.54	0.24	2.06	1.71	-20.8	30.2	1.42	0.185	
21 31 52.555	-01 01 52.02	*	18.44	20.22	1.78	0.14	0.14	4.09	4.41	-21.8	31.2	2.00	0.390	I
21 39 50.995	-08 04 54.67	gR	12.64	13.39	0.75	0.11	0.39	5.83	11.41	-24.1	29.8	-0.25	0.051	I
21 45 08.153	-00 23 41.21	gR	18.68	20.64	1.96	0.18	0.39	1.70	1.85	-20.1	30.3	1.82	0.226	
22 06 02.534	-08 21 06.44	gR	11.82	12.34	0.52	0.09	1.20	2.33	2.88	-25.7	29.5	-1.28	0.067	
22 23 40.975	-08 24 57.95	gB	18.76	20.41	1.65	0.14	0.08	5.53	5.37	-21.2	31.1	2.19	0.330	
22 27 07.151	-00 18 36.05	*	17.64	18.57	0.93	0.24	0.44	1.03	1.81	-21.0	29.8	1.00	0.130	
22 51 22.146	-08 57 23.06	gR	16.69	17.72	1.03	0.12	0.82	1.47	1.67	-20.7	29.4	0.64	0.080	
22 52 13.528	-08 57 46.89	gR	17.87	19.54	1.67	0.12	0.71	1.06	1.52	-21.5	30.3	1.29	0.250	
23 28 21.736	-11 07 03.01	gB	18.19	19.50	1.31	0.08	0.35	6.13	5.82	-21.3	30.9	1.89	0.231	I
23 43 10.762	-09 25 35.19	gR	18.33	18.91	0.58	0.08	0.11	1.10	0.96	-19.8	29.3	0.93	0.089	
23 44 13.563	+00 48 14.20	gB	11.25	12.66	1.42	0.07	1.32	2.62	8.08	-24.7	29.7	-0.69	0.050	CJ
23 46 29.631	-00 16 40.57	gR	18.49	19.96	1.47	0.11	1.17	1.90	1.81	-21.2	30.5	1.56	0.263	
23 48 01.656	-09 11 55.28	gR	14.33	13.54	-0.79	0.09	0.35	3.91	4.92	-25.2	30.0	-0.57	0.093	I
00 08 04.122	-01 29 16.58	*	18.13	19.93	1.80	0.10	0.96	1.90	1.82	-21.6	30.6	1.54	0.313	
00 27 16.201	-01 46 48.20	gR	9.33	10.06	0.73	0.07	0.56	7.79	18.42	-26.7	29.8	-1.38	0.037	o,I
00 33 44.963	-02 10 09.28	gB	18.28	19.38	1.10	0.08	0.50	15.48	15.28	-20.6	31.0	2.25	0.162	
00 46 15.395	-08 32 31.34	*	17.89	19.22	1.32	0.09	0.32	2.37	3.13	-22.3	30.8	1.47	0.307	
00 58 43.491	-11 14 04.15	gR	18.50	19.30	0.81	0.09	0.97	1.87	1.41	-21.6	30.4	1.29	0.240	I
01 09 16.941	-08 12 01.25	*	18.84	20.60	1.76	0.15	0.38	1.59	1.12	-21.2	30.6	1.72	0.348	
01 09 48.881	-10 28 25.02	gR	18.86	20.53	1.68	0.07	0.52	1.85	2.14	-19.9	30.3	1.85	0.199	
01 20 31.781	-08 32 02.84	gR	18.11	19.97	1.86	0.12	0.66	10.03	13.39	-20.8	31.2	2.41	0.224	
01 39 42.155	-00 06 18.63	gR	17.72	19.14	1.42	0.09	0.61	37.33	38.78	-21.3	31.5	2.55	0.197	
01 46 13.342	+01 36 01.19	gR	17.53	18.92	1.39	0.07	0.25	13.47	13.25	-21.9	31.2	2.00	0.230	o
01 58 42.775	-00 30 41.19	*	18.35	19.81	1.47	0.06	0.23	1.97	2.13	-21.3	30.5	1.55	0.266	
02 01 47.597	+01 34 04.79	*	18.09	19.44	1.35	0.08	0.68	2.00	1.53	-20.5	30.0	1.39	0.157	
02 03 41.942	-02 42 14.02	gR	18.59	19.54	0.95	0.07	0.45	14.76	15.72	-21.0	31.2	2.32	0.200	I
02 17 47.058	+00 43 21.48	gR	18.29	20.22	1.93	0.11	0.96	1.83	1.78	-21.0	30.5	1.64	0.275	
02 32 47.492	+00 40 40.85	gR	13.98	13.79	-0.20	0.07	0.59	1.16	0.96	-21.9	28.1	-1.08	0.023	
02 49 40.198	-08 28 04.39	gR	18.69	20.53	1.85	0.08	0.58	4.47	4.41	-20.6	30.9	2.15	0.271	
03 17 29.602	-01 10 47.20	gR	17.38	17.71	0.33	0.18	0.52	1.22	1.86	-22.2	30.0	0.67	0.151	

Note. — Table columns are same as Table 1.

Table 3
BL Lacertae Objects in FBQS Candidate List

RA (1)	Dec (2)	Cl (3)	R (4)	B (5)	B-R (6)	A(R) (7)	Sep (8)	S_p (9)	S_i (10)	M_B (11)	$\log L_R$ (12)	$\log R^*$ (13)	z (14)	Notes (15)
21 29 40.691	+00 35 27.86	gR	18.81	20.00	1.18	0.12	0.25	5.86	5.92	-22.2	31.4	2.04	0.425	
21 34 10.335	-01 53 17.39	*	18.25	19.83	1.58	0.15	0.32	1498.44	1619.87	···	···	4.49	···	o
21 56 14.755	-00 37 04.58	*	18.62	20.51	1.89	0.32	0.19	165.65	170.17	···	···	3.78	···	
21 56 50.339	-08 55 35.36	*	18.24	19.73	1.49	0.09	0.19	20.45	21.49	···	···	2.57	···	
22 04 45.256	+00 31 42.32	*	16.73	18.35	1.62	0.15	0.61	2.94	3.03	-26.6	32.1	0.98	1.330	
22 11 08.341	-00 03 02.52	*	17.53	18.91	1.38	0.17	0.16	15.25	16.89	···	···	2.14	···	X
22 17 25.998	-09 07 05.21	gR	12.76	13.15	0.39	0.19	0.79	1.11	3.73	-25.7	29.9	-0.85	0.095	
22 25 58.839	-01 45 12.07	gR	18.08	18.73	0.65	0.13	0.17	8.75	9.01	···	···	1.79	···	?
22 27 58.139	+00 37 05.49	*	17.92	18.67	0.75	0.17	0.18	99.12	103.79	···	···	2.83	···	
22 47 30.200	+00 00 06.68	*	18.08	19.53	1.45	0.26	0.10	183.71	190.56	···	···	3.44	···	
23 11 16.998	-10 38 49.36	gR	18.40	19.40	1.00	0.09	0.31	1108.35	1161.71	···	···	4.17	···	
23 34 48.349	-08 34 37.91	gB	18.89	19.80	0.91	0.08	0.73	1.00	1.20	-20.8	30.1	1.30	0.208	?
23 41 25.023	-01 52 24.53	gR	18.47	19.62	1.15	0.08	0.44	34.39	36.83	···	···	2.76	···	?
23 56 04.010	-00 23 53.86	gR	17.98	19.45	1.47	0.09	0.32	5.48	5.18	-21.8	31.0	1.81	0.283	
00 11 39.679	-00 28 27.94	gR	11.49	12.19	0.70	0.12	1.03	1.56	9.63	-25.6	29.9	-0.81	0.059	
00 50 41.303	-09 29 05.49	*	15.69	17.47	1.78	0.09	0.26	802.52	893.68	···	···	3.28	···	o,X
01 00 58.190	-00 55 47.84	*	18.71	19.75	1.03	0.09	0.11	31.17	31.81	···	···	2.74	···	$z > 1.236$
01 05 40.749	-00 33 14.07	*	17.59	19.41	1.82	0.10	0.24	4.59	4.84	-25.2	32.2	1.62	1.178	?
01 27 11.072	-01 51 53.85	*	18.37	19.31	0.94	0.11	0.51	9.69	10.62	···	···	2.09	···	
01 27 16.304	-08 21 29.23	gB	18.27	17.07	-1.19	0.08	0.13	168.57	172.23	···	···	2.41	···	
02 43 02.927	+00 46 27.33	*	18.30	20.05	1.75	0.08	0.44	28.52	31.38	-22.1	32.1	2.79	0.409	
02 53 15.611	-01 24 05.35	*	17.04	18.48	1.44	0.16	0.29	31.34	32.68	···	···	2.25	···	
03 04 33.974	-00 54 04.15	gR	17.76	19.13	1.37	0.22	0.77	19.47	23.28	···	···	2.36	···	

Note. — Table columns are the same as in Table 1.

Table 4
H II Region Galaxies in FBQS Candidate List

RA (1)	Dec (2)	Cl (3)	R (4)	B (5)	B-R (6)	A(R) (7)	Sep (8)	S_p (9)	S_i (10)	M_B (11)	$\log L_R$ (12)	$\log R^*$ (13)	z (14)	Notes (15)
21 22 20.646	-00 00 46.38	gR	18.28	19.86	1.59	0.15	0.75	1.48	0.75	-21.5	30.5	1.40	0.297	
21 41 55.403	-08 49 15.63	gR	17.46	18.71	1.25	0.10	0.13	1.04	0.78	-22.0	30.1	0.80	0.220	
22 48 14.954	-01 09 23.14	gR	18.38	20.23	1.84	0.27	0.69	1.14	1.11	-19.3	29.6	1.46	0.128	
23 27 14.545	-10 23 17.75	gR	12.79	12.57	-0.22	0.08	0.30	1.41	2.25	-25.4	29.3	-1.29	0.065	I
23 30 54.903	-00 00 40.14	gR	18.53	20.38	1.85	0.12	0.12	2.22	2.68	-19.8	30.3	1.89	0.174	
23 56 59.633	-02 05 00.85	*	12.04	12.84	0.80	0.10	0.15	1.05	1.23	-23.0	28.2	-1.43	0.024	I
00 06 18.889	-08 53 33.05	gR	13.44	13.09	-0.35	0.10	0.95	1.06	1.98	-25.0	29.3	-1.14	0.068	
00 06 39.951	-01 31 40.48	gB	18.12	19.28	1.16	0.11	0.29	3.43	3.43	-21.1	30.5	1.55	0.193	
00 14 55.103	+00 15 07.74	gR	10.98	11.04	0.06	0.07	0.58	1.25	2.57	-25.8	28.9	-1.84	0.039	I
00 18 50.872	-10 22 36.92	gR	11.30	11.37	0.06	0.10	0.50	24.53	34.82	-24.7	29.8	-0.57	0.027	
00 27 22.574	-08 42 18.80	gB	18.44	19.68	1.24	0.10	0.30	3.65	3.53	-19.6	30.0	1.75	0.115	
00 35 42.918	+01 13 01.00	*	12.53	13.04	0.51	0.06	0.49	1.39	3.54	-23.9	29.1	-0.90	0.041	I
00 39 35.824	-09 11 39.80	*	9.03	10.08	1.06	0.09	0.58	2.58	5.64	-24.8	28.5	-1.87	0.016	I
00 40 10.542	-10 26 25.62	gR	12.00	12.23	0.23	0.09	0.92	1.52	3.73	-23.9	28.8	-1.20	0.028	I
00 43 36.314	-09 25 48.16	gR	13.64	13.71	0.07	0.10	0.32	1.20	0.88	-23.7	28.8	-1.10	0.050	I
00 52 08.954	-02 13 06.61	gR	10.18	10.28	0.09	0.12	0.97	4.11	6.05	-29.3	30.4	-1.79	0.134	I
01 13 12.996	+01 16 50.78	gR	11.99	12.58	0.60	0.09	0.92	1.63	4.67	-24.6	29.3	-0.96	0.045	I
01 42 07.217	-00 29 41.31	gR	14.61	14.40	-0.21	0.08	0.64	1.46	1.65	-24.5	29.6	-0.70	0.100	
02 03 54.100	-03 53 00.56	gR	12.35	12.13	-0.22	0.07	1.03	2.32	6.85	-24.9	29.4	-0.98	0.042	I
02 04 55.699	-02 08 50.95	gR	18.36	18.39	0.03	0.08	0.39	1.38	0.87	-21.8	30.0	0.81	0.177	I
02 34 02.807	-01 24 58.51	*	18.40	19.78	1.39	0.08	1.15	1.21	1.10	-21.0	30.2	1.29	0.232	
03 07 49.481	-00 47 00.68	gB	11.32	11.85	0.53	0.18	0.31	1.27	2.48	-23.4	28.3	-1.53	0.019	
03 19 17.173	-00 58 10.96	gR	13.97	13.52	-0.44	0.16	0.45	1.04	1.72	-24.1	29.1	-1.02	0.054	

Note. — Table columns are same as Table 1.

Table 5
Passive Galaxies in FBQS Candidate List

RA (1)	Dec (2)	Cl (3)	R (4)	B (5)	B-R (6)	A(R) (7)	Sep (8)	S_p (9)	S_i (10)	M_B (11)	$\log L_R$ (12)	$\log R^*$ (13)	z (14)	Notes (15)
21 20 30.602	-01 38 40.45	gR	18.75	19.99	1.23	0.13	0.23	6.30	6.27	-21.7	31.2	2.07	0.334	
22 26 02.367	+00 09 30.81	gR	18.38	20.23	1.85	0.22	0.05	2.13	1.59	-21.1	30.6	1.71	0.290	
22 26 34.074	-09 01 06.47	*	18.13	19.43	1.30	0.13	0.60	1.73	1.72	-22.0	30.5	1.30	0.299	I
23 18 49.658	-09 35 15.52	gR	18.85	20.56	1.71	0.08	0.46	4.07	3.93	-20.3	30.7	2.13	0.236	
23 42 03.314	-08 51 28.17	gR	18.84	20.55	1.71	0.08	0.17	1.88	2.85	···	···	2.02	···	o
23 45 57.122	-10 28 48.20	gR	17.86	18.81	0.95	0.09	0.42	11.49	12.39	-22.8	31.5	1.90	0.330	
23 47 12.620	-10 34 00.38	gR	18.66	20.17	1.51	0.09	0.33	2.88	2.91	-21.2	30.7	1.82	0.289	
23 50 48.109	-11 21 43.78	gR	17.38	19.10	1.72	0.07	0.82	1.82	1.82	-22.3	30.6	1.19	0.302	
00 33 30.206	-08 56 47.04	*	18.79	20.59	1.80	0.10	0.19	12.82	13.88	···	···	2.72	···	
00 57 52.528	-09 17 14.82	gB	18.81	19.37	0.56	0.11	0.62	11.30	11.50	-20.4	30.7	2.12	0.145	
01 16 26.404	+01 30 23.45	gB	18.64	20.65	2.00	0.10	0.33	2.87	3.48	-20.4	30.7	2.09	0.256	
02 02 24.786	-01 45 10.74	gR	16.88	18.18	1.31	0.07	0.62	65.62	72.98	-22.4	31.9	2.44	0.212	
02 09 15.945	-04 47 17.55	gR	17.73	18.71	0.98	0.06	0.46	3.81	3.72	-21.3	30.4	1.38	0.165	I
02 28 22.543	+01 30 25.24	gR	18.61	20.53	1.92	0.09	0.47	1.91	1.98	-20.6	30.5	1.80	0.266	
03 03 52.894	+00 24 55.44	gB	10.92	11.48	0.56	0.22	0.19	4.68	7.27	-25.6	29.5	-1.21	0.043	
03 12 02.518	-00 04 42.32	gB	11.07	11.75	0.68	0.19	0.81	8.59	10.03	-25.1	29.5	-0.96	0.038	
03 19 09.642	-00 19 17.05	gR	18.54	19.87	1.33	0.18	0.55	2.10	1.99	-23.3	31.3	1.51	0.636	

Note. — Table columns are same as Table 1.

Table 6
Stars in FBQS Candidate List

RA (1)	Dec (2)	Cl (3)	R (4)	B (5)	B-R (6)	A(R) (7)	Sep (8)	S_p (9)	S_i (10)	Notes (11)
21 03 36.181	-07 15 34.78	*	17.63	18.94	1.31	0.25	0.93	1.32	0.83	
21 12 27.627	-07 19 31.73	*	17.98	19.58	1.60	0.40	0.33	1.12	10.29	
21 13 57.288	-06 41 35.13	*	11.74	12.51	0.77	0.33	0.70	1.15	1.44	
21 16 11.898	-06 28 30.09	gR	17.74	18.85	1.11	0.37	0.44	13.79	14.87	
21 17 58.907	-07 46 11.55	*	14.19	15.25	1.05	0.39	0.90	3.16	3.39	
21 29 26.165	+00 24 35.38	*	15.36	17.07	1.70	0.12	0.09	4.29	4.46	
21 31 57.191	+01 30 25.51	*	16.72	18.51	1.79	0.14	0.67	6.51	11.17	
21 35 20.147	-01 04 26.03	*	18.60	19.73	1.13	0.13	1.37	2.66	3.53	CJ
21 43 45.622	+01 06 56.50	*	17.20	18.15	0.95	0.14	1.10	1.13	1.10	
21 45 43.184	-08 15 47.40	*	18.17	19.40	1.23	0.12	1.16	4.01	8.02	
21 47 20.228	+00 42 00.94	*	15.79	17.15	1.37	0.34	0.27	1.38	1.86	
22 05 01.002	-07 18 07.73	*	18.24	19.44	1.21	0.12	0.75	5.49	5.39	
22 05 32.591	-01 33 25.37	*	17.26	18.29	1.02	0.40	0.38	15.99	16.66	
22 10 43.685	-08 25 29.41	*	17.34	19.06	1.72	0.15	1.01	1.29	3.61	
22 12 41.650	+00 36 35.81	*	15.92	17.19	1.27	0.12	2.68	2.14	2.52	DBL
22 16 10.096	-00 08 23.00	*	16.65	17.82	1.17	0.21	1.19	1.31	1.21	
22 51 21.141	+01 24 14.51	*	16.25	18.11	1.86	0.22	1.14	1.14	1.14	
23 06 03.470	-10 00 42.86	*	17.34	18.38	1.04	0.11	1.18	1.85	1.76	
23 26 42.929	-02 09 17.02	*	17.43	18.64	1.21	0.14	1.15	1.49	102.10	
23 45 47.758	-10 50 30.90	*	17.89	18.59	0.71	0.08	1.06	7.39	8.09	
23 53 08.273	-01 40 33.31	gR	17.69	19.16	1.47	0.10	7.30	1.30	3.81	DBL
00 01 11.195	-00 20 11.57	*	17.87	18.40	0.53	0.10	0.08	23.28	25.00	
00 12 57.945	+00 41 47.21	*	14.52	16.02	1.50	0.08	1.17	1.13	0.81	
00 36 50.884	-02 11 47.92	*	15.34	16.31	0.98	0.08	0.53	4.13	22.67	
00 38 59.253	+00 18 42.20	*	17.03	18.84	1.81	0.05	0.32	1.93	2.01	
01 14 19.164	-00 08 07.23	*	18.47	19.19	0.72	0.08	1.16	1.21	1.27	
01 22 05.490	+00 30 45.31	*	17.00	18.18	1.18	0.10	0.96	1.77	1.09	
01 50 39.766	-01 08 21.40	gB	16.97	18.76	1.78	0.08	0.43	1.82	1.96	
02 03 59.582	-09 00 02.68	*	15.08	16.05	0.96	0.07	0.56	1.41	1.97	
02 09 01.679	-03 07 12.20	*	16.62	17.76	1.14	0.07	1.11	7.43	57.93	
02 58 00.277	+01 13 32.67	*	18.03	18.59	0.56	0.25	1.07	11.95	12.38	
03 13 41.345	+01 22 57.22	*	18.19	18.67	0.49	0.35	0.33	1.14	0.63	

Note. — Table columns are same as Table 1, except that redshift, absolute magnitudes, etc., are omitted for these Galactic objects.

Table 7
Objects Without Spectra in FBQS Candidate List

RA (1)	Dec (2)	Cl (3)	R (4)	B (5)	B-R (6)	A(R) (7)	Sep (8)	S_p (9)	S_i (10)	P(Q) (11)	Notes (12)
21 26 27.266	+01 23 21.44	*	18.86	19.51	0.65	0.12	0.83	1.37	1.74	0.87	
21 57 55.635	-07 46 53.17	*	17.87	18.78	0.91	0.11	0.56	1.08	17.33	0.14	
22 09 08.252	-00 55 59.06	gR	18.61	19.90	1.29	0.27	0.32	20.88	21.16	0.65	
22 11 09.861	-00 23 27.20	gR	18.42	20.26	1.84	0.30	0.65	29.31	38.84	0.51	
22 20 35.227	-07 49 47.34	gB	17.79	17.11	-0.68	0.20	0.19	10.46	12.92	0.42	
22 24 46.000	-08 46 56.42	*	18.84	19.38	0.55	0.13	0.11	34.93	36.36	0.88	
22 26 52.940	-00 07 15.07	gR	18.02	19.63	1.61	0.21	1.09	1.90	1.51	0.27	
22 35 16.241	-00 58 49.77	*	18.85	19.43	0.58	0.14	0.04	2.91	2.28	0.88	
22 38 39.967	+00 45 09.13	*	18.73	19.58	0.85	0.19	0.09	3.94	3.46	0.87	
22 39 06.327	+01 08 06.73	*	18.82	19.18	0.36	0.19	0.35	11.59	11.92	0.88	
22 40 06.131	+01 27 32.32	gB	18.85	20.05	1.20	0.22	0.51	18.69	21.67	0.87	
22 41 53.456	-01 55 44.27	*	18.57	19.19	0.62	0.14	0.11	15.20	15.49	0.88	
22 43 13.195	-01 05 53.15	*	18.66	19.75	1.09	0.15	0.37	7.35	9.64	0.87	
22 45 23.499	-00 36 21.93	*	18.52	19.32	0.80	0.17	0.60	1.36	1.80	0.87	
22 45 41.331	-01 54 41.54	gB	18.54	20.49	1.95	0.18	0.74	1.16	0.75	0.11	
22 49 29.254	-00 09 16.40	*	18.55	19.20	0.65	0.28	1.04	3.99	3.88	0.88	
23 07 45.140	-00 45 42.56	*	18.87	19.42	0.55	0.15	0.29	6.17	7.86	0.88	
23 07 52.523	-10 03 13.98	*	18.78	19.26	0.48	0.09	0.34	58.08	59.95	0.88	
23 39 03.835	-09 12 21.00	gB	18.78	20.52	1.74	0.07	0.30	4.34	4.06	0.44	
23 50 50.719	-00 28 48.53	gR	18.30	19.25	0.95	0.08	0.29	11.57	12.50	0.87	
23 53 13.634	-00 50 23.35	*	18.74	19.31	0.57	0.08	0.14	1.15	0.59	0.88	
23 53 41.794	+00 18 01.97	*	18.55	19.61	1.06	0.11	0.73	1.13	1.17	0.87	
23 53 56.860	-00 52 14.78	*	18.50	19.33	0.82	0.08	0.16	12.14	12.91	0.87	
23 54 37.275	-08 35 59.50	*	18.68	18.69	0.01	0.09	0.11	27.54	29.18	0.88	
23 55 48.174	-09 41 36.57	gB	18.68	20.63	1.95	0.10	0.98	1.16	1.02	0.11	
23 55 54.660	-02 02 46.00	*	18.81	19.53	0.72	0.09	0.69	1.66	1.39	0.88	
23 56 11.918	-01 51 11.60	*	18.63	19.30	0.67	0.10	0.64	1.55	1.10	0.87	
23 57 25.140	-01 52 15.60	*	18.63	19.77	1.14	0.12	0.33	283.61	291.48	0.87	
23 58 22.967	-10 04 10.36	gB	18.79	20.65	1.86	0.10	1.00	2.04	2.19	0.11	
23 58 29.702	-01 03 04.50	gR	18.24	19.68	1.45	0.10	0.54	5.20	5.21	0.27	
23 58 39.620	+00 29 05.59	*	18.55	19.10	0.56	0.09	1.16	1.72	2.64	0.86	
23 59 46.813	+01 02 27.96	gR	18.81	20.14	1.33	0.07	0.38	23.01	24.92	0.67	
00 00 28.828	-10 27 55.39	*	18.86	19.64	0.78	0.11	0.21	2.40	2.23	0.88	
00 01 21.522	-00 11 40.75	*	18.63	20.33	1.70	0.09	0.89	39.38	80.62	0.36	
00 02 57.196	-00 24 47.51	*	18.59	20.34	1.75	0.10	0.32	124.90	159.13	0.59	
00 03 09.465	+01 24 28.13	gR	18.84	20.81	1.97	0.09	1.06	2.31	2.46	0.11	
00 09 26.932	-11 08 05.02	*	18.68	19.89	1.21	0.09	0.60	1.39	1.17	0.77	
00 13 05.002	-01 05 49.35	*	18.47	19.14	0.68	0.11	0.13	16.64	17.78	0.87	
00 16 07.013	-09 11 45.23	gR	18.80	20.75	1.94	0.12	0.64	1.42	3.48	0.11	
00 17 35.706	-01 13 25.15	*	18.64	20.02	1.38	0.14	0.15	6.77	7.11	0.84	
00 23 34.092	-09 26 24.80	*	18.77	19.04	0.27	0.14	0.60	1.47	1.13	0.88	
00 42 53.469	+00 42 46.20	*	18.81	20.72	1.91	0.05	0.49	4.08	5.31	0.11	
00 49 33.540	-01 29 30.89	*	18.76	20.39	1.63	0.14	0.24	2.48	2.01	0.80	
00 50 04.902	-00 14 23.50	gB	18.90	20.51	1.61	0.09	0.83	1.42	2.66	0.11	
01 25 23.855	-10 26 15.10	*	18.72	19.26	0.54	0.08	0.49	2.16	1.95	0.88	
01 39 59.213	+01 07 37.63	*	18.74	19.71	0.98	0.08	0.41	8.09	7.84	0.87	
01 43 35.141	-01 34 56.00	*	18.81	19.42	0.61	0.08	0.14	7.59	7.62	0.88	
01 50 10.838	-01 44 19.03	gB	18.84	19.01	0.18	0.09	0.96	2.38	4.37	0.78	
01 52 05.458	+00 44 53.72	gB	18.83	20.10	1.27	0.08	0.82	1.08	1.01	0.21	
01 52 43.185	+00 20 40.26	gR	18.71	19.95	1.24	0.10	0.29	91.69	172.27	0.86	
01 53 29.760	-00 22 14.32	*	18.69	19.44	0.75	0.09	0.09	14.98	15.31	0.87	
01 54 54.370	-00 07 23.06	gR	18.63	19.20	0.57	0.08	0.41	259.07	265.59	0.87	
01 55 16.068	-02 13 25.04	*	18.77	19.45	0.68	0.07	0.15	10.25	10.36	0.87	
01 56 33.576	+00 30 45.85	*	18.62	19.40	0.78	0.08	0.08	3.95	4.35	0.87	
01 57 48.962	+01 19 39.84	*	18.28	18.72	0.44	0.07	0.72	4.05	4.69	0.88	
02 00 33.000	-03 24 56.02	*	18.79	19.06	0.27	0.07	1.09	1.05	1.21	0.88	
02 01 06.463	-06 48 57.10	gR	9.19	10.46	1.27	0.07	0.90	3.33	2.85	0.11	I
02 02 01.128	-02 49 31.16	*	18.85	20.79	1.94	0.07	0.62	1.58	1.72	0.11	
02 05 07.429	-01 12 14.94	*	18.27	19.44	1.17	0.07	0.26	15.95	17.32	0.87	
02 09 07.010	-01 10 34.20	*	18.76	20.25	1.50	0.09	0.80	1.69	1.87	0.25	
02 09 57.103	+00 04 24.86	gB	18.59	20.21	1.63	0.07	0.98	1.29	0.83	0.11	
02 10 06.576	-03 25 44.42	gR	18.53	20.46	1.92	0.07	1.17	2.93	4.27	0.12	
02 11 17.446	-02 03 45.94	gB	18.74	20.74	2.00	0.08	0.25	5.02	4.33	0.11	
02 13 11.710	-05 01 01.87	*	18.83	20.18	1.35	0.05	1.03	30.24	32.56	0.87	
02 17 13.390	-00 45 26.95	*	18.77	18.96	0.19	0.10	0.22	4.77	4.64	0.88	
02 18 40.385	-00 20 19.25	gR	18.65	20.43	1.77	0.09	0.16	6.13	6.02	0.20	
02 22 43.272	+00 06 34.88	*	18.71	20.55	1.85	0.11	1.15	1.39	0.93	0.11	
02 28 10.583	-01 48 52.82	gR	18.40	19.99	1.60	0.08	1.00	1.03	1.07	0.11	
02 29 58.482	-00 57 35.50	*	18.77	20.25	1.47	0.09	0.10	2.05	2.12	0.77	
02 31 01.173	-00 49 43.98	gB	18.75	19.70	0.95	0.08	0.09	18.15	18.78	0.87	
02 40 31.300	-01 38 56.36	*	18.72	19.13	0.41	0.09	0.14	3.73	3.78	0.88	
02 42 24.037	+01 04 53.33	*	18.71	19.74	1.03	0.11	0.31	2.56	3.15	0.87	
02 44 10.922	-00 56 53.80	gR	18.89	20.78	1.89	0.07	0.24	2.88	2.87	0.15	
02 48 02.546	-07 19 15.93	gR	18.89	19.41	0.52	0.10	0.26	28.05	35.46	0.87	
03 13 22.482	-00 10 18.86	gR	18.54	20.02	1.48	0.25	0.78	1.16	2.04	0.11	

Note. — Table columns are same as Table 6, with the addition of Col. 11. $P(Q)$ is the probability that the candidate is a quasar, computed as described in Paper II. All source parameters including color were used.

Table 8
Broad Absorption-Line Quasars

RA (1)	Dec (2)	M_B (3)	$\log L_R$ (4)	$\log R^*$ (5)	z (6)	BALnicity[a] (7)	Notes (8)
21 24 10.271	-07 22 19.95	-27.7	33.0	1.49	1.760	800	HiBAL
23 00 11.749	-10 21 44.02	-27.7	34.3	2.74	2.300	0	HiBAL?
23 36 11.627	-09 54 27.05	-27.1	32.1	0.80	1.760	100	HiBAL
23 47 11.497	-10 37 42.18	-28.0	32.0	0.33	1.780	9000	LoBAL
00 14 38.279	-01 07 50.31	-25.7	32.0	1.30	1.800	0	LoBAL?
00 46 13.548	+01 04 25.78	-28.0	32.5	0.80	2.150	2100	o,HiBAL
01 28 41.876	-00 33 16.79	-26.2	32.2	1.31	1.650	2700	HiBAL
01 35 15.239	-02 13 49.26	-28.0	33.2	1.56	1.820	1900	HiBAL
01 40 18.199	-01 38 05.94	-28.2	32.2	0.46	2.240	1400	o,HiBAL
01 48 12.829	-00 51 09.01	-26.5	32.4	1.32	1.820	6800	HiBAL
01 53 45.346	-10 08 40.06	-26.5	32.5	1.46	1.900	600	HiBAL
02 00 22.031	-08 45 11.76	-26.2	32.8	1.85	1.930	2300	HiBAL
02 21 00.743	-01 22 12.16	-25.5	31.8	1.10	1.210	50[b]	LoBAL
02 56 25.641	-01 19 11.51	-27.7	33.5	1.99	2.490	250	HiBAL

[a]Table columns 1–6 and 8 are from Table 1. Column 7 is the "BALnicity index" (Weymann et al. 1991), which if non-zero indicates high confidence that the absorption is a true broad-absorption line rather than associated absorption.

[b]BALnicity was computed from Mg II, which generally is narrower than the high ionization lines.

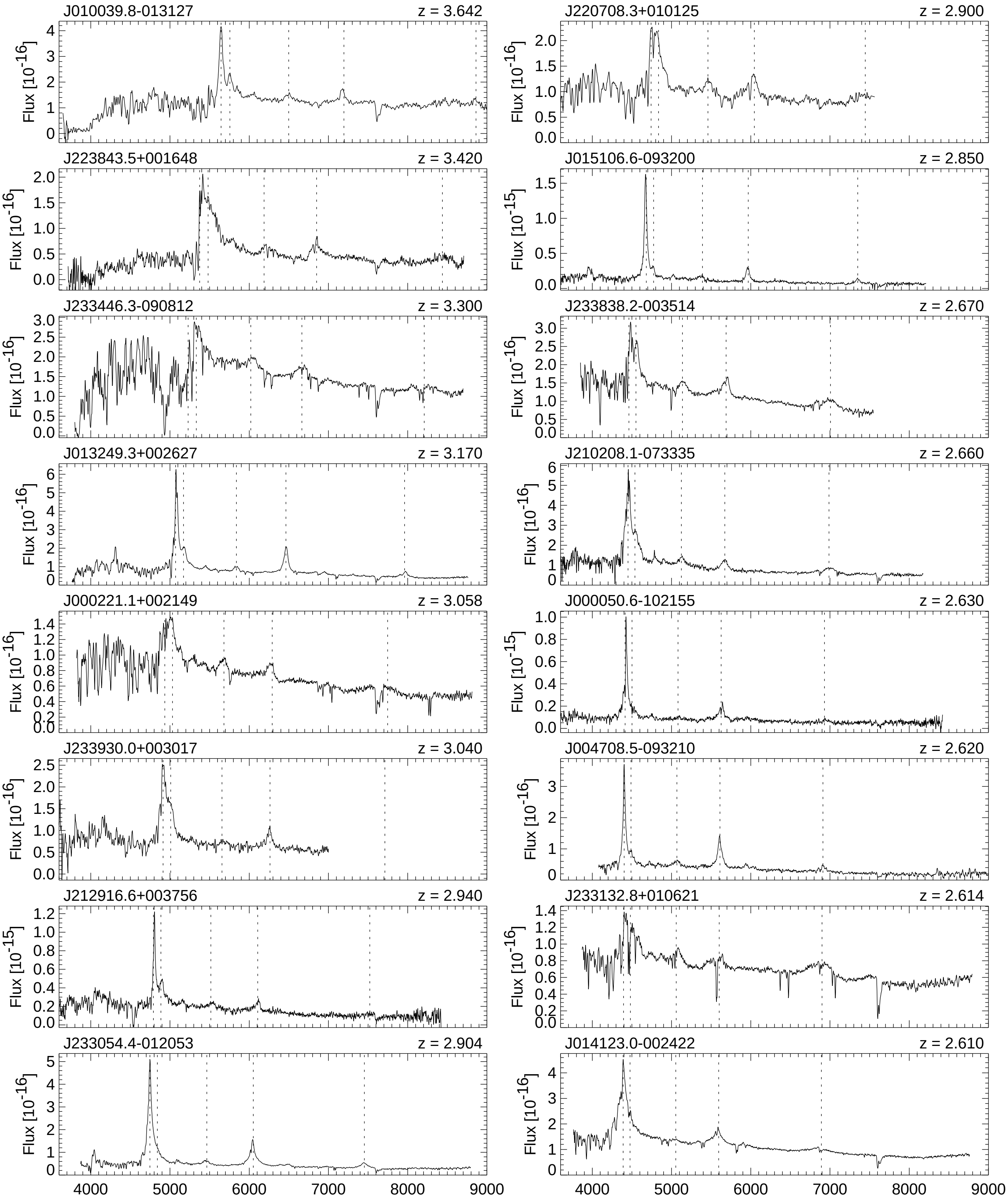

FIG. 9.— Spectra of FBQS candidates identified as quasars, sorted by decreasing redshift. The dotted lines show expected positions of prominent emission lines: Lyα 1216, N V 1240, Si IV 1400, C IV 1550, C III] 1909, Mg II 2800, Hδ 4102, Hγ 4341, Hβ 4862, [O III] 4959, [O III] 5007, Hα 6563. Note that most of the spectra have atmospheric A and B band absorption at $\sim$ 6880 Å and 7620 Å.

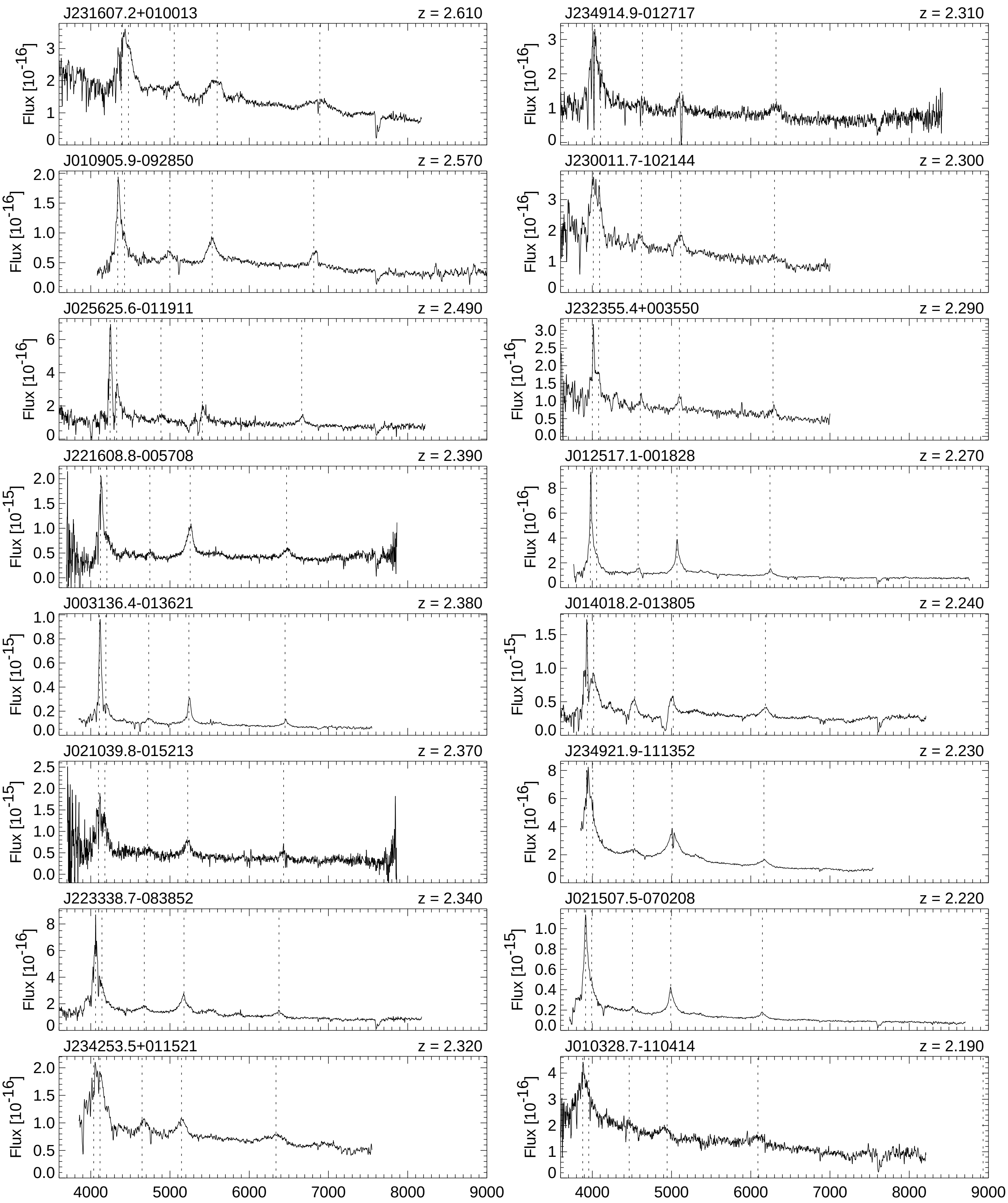

FIG. 9B.— *Continued.* Spectra of FBQS quasars.

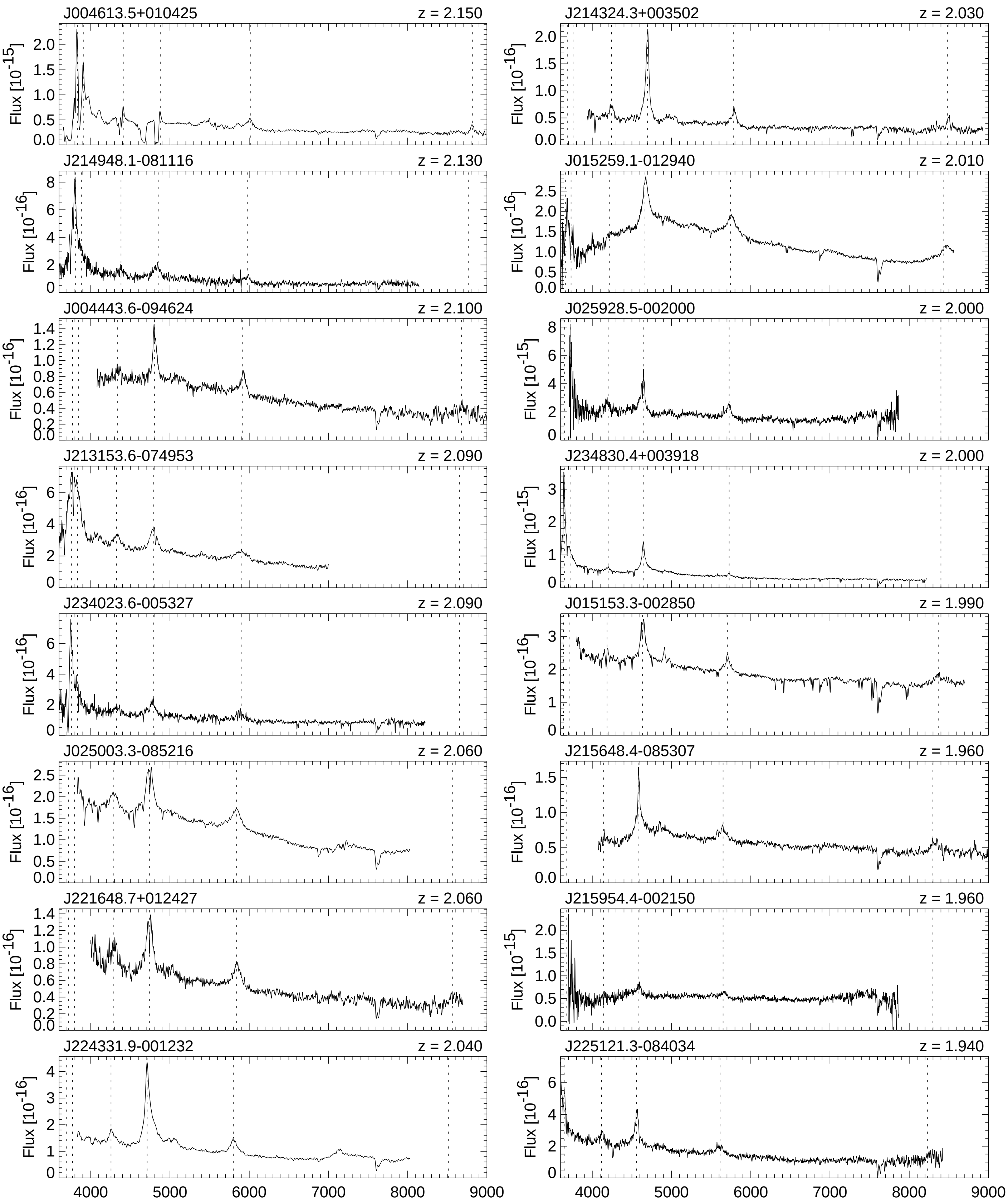

FIG. 9C.— *Continued.* Spectra of FBQS quasars.

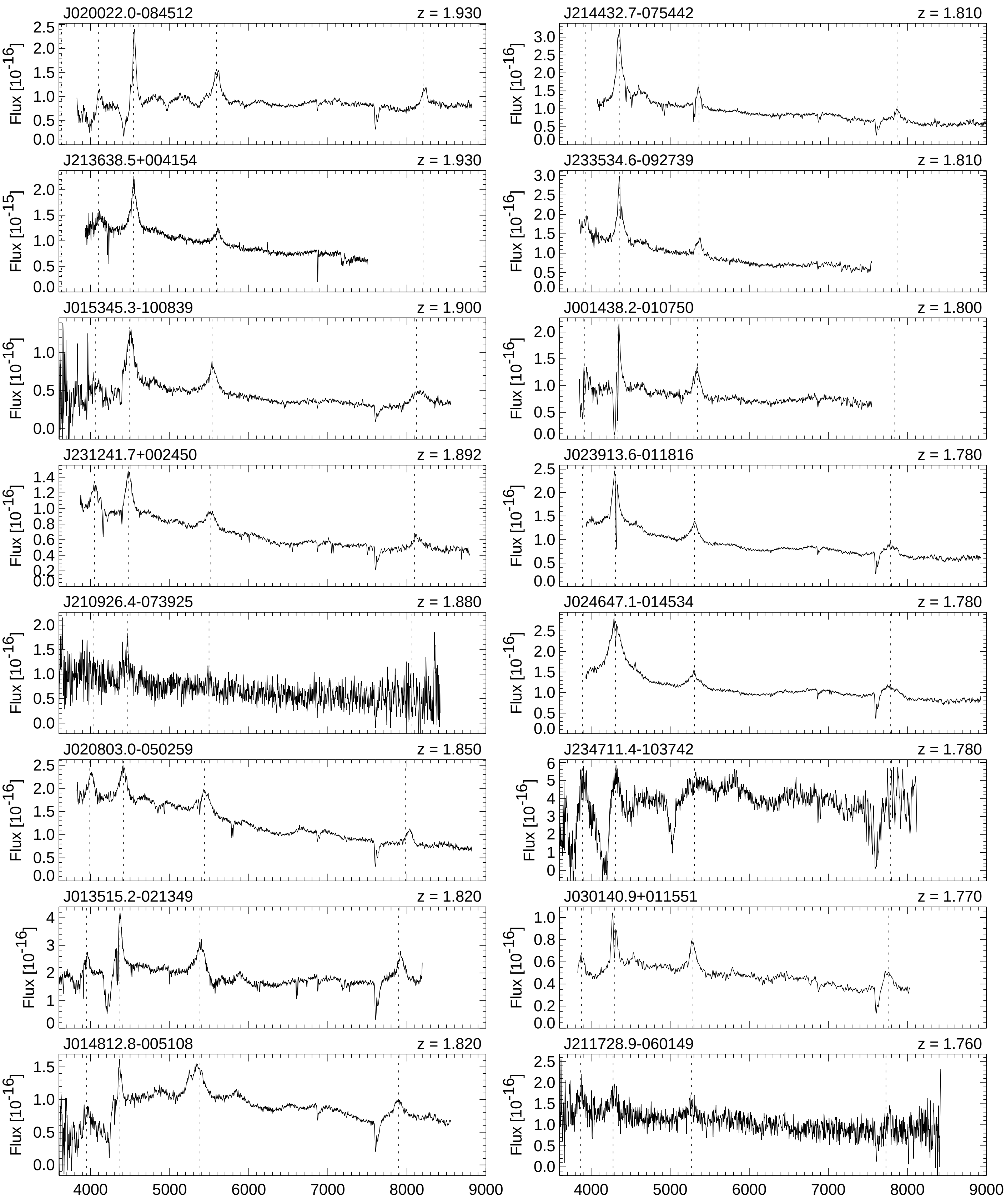

Fig. 9d.— *Continued.* Spectra of FBQS quasars.

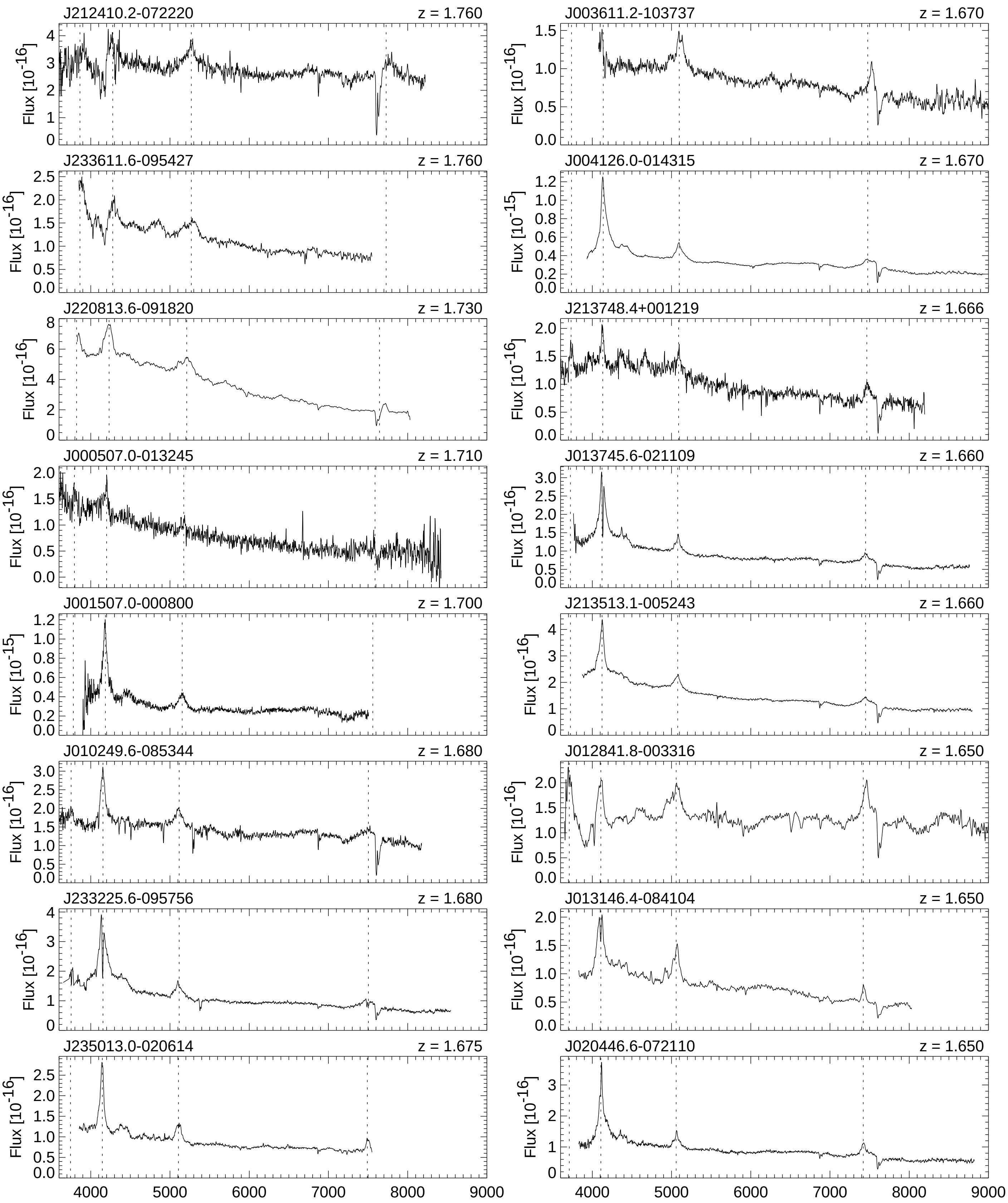

FIG. 9E.— *Continued.* Spectra of FBQS quasars.

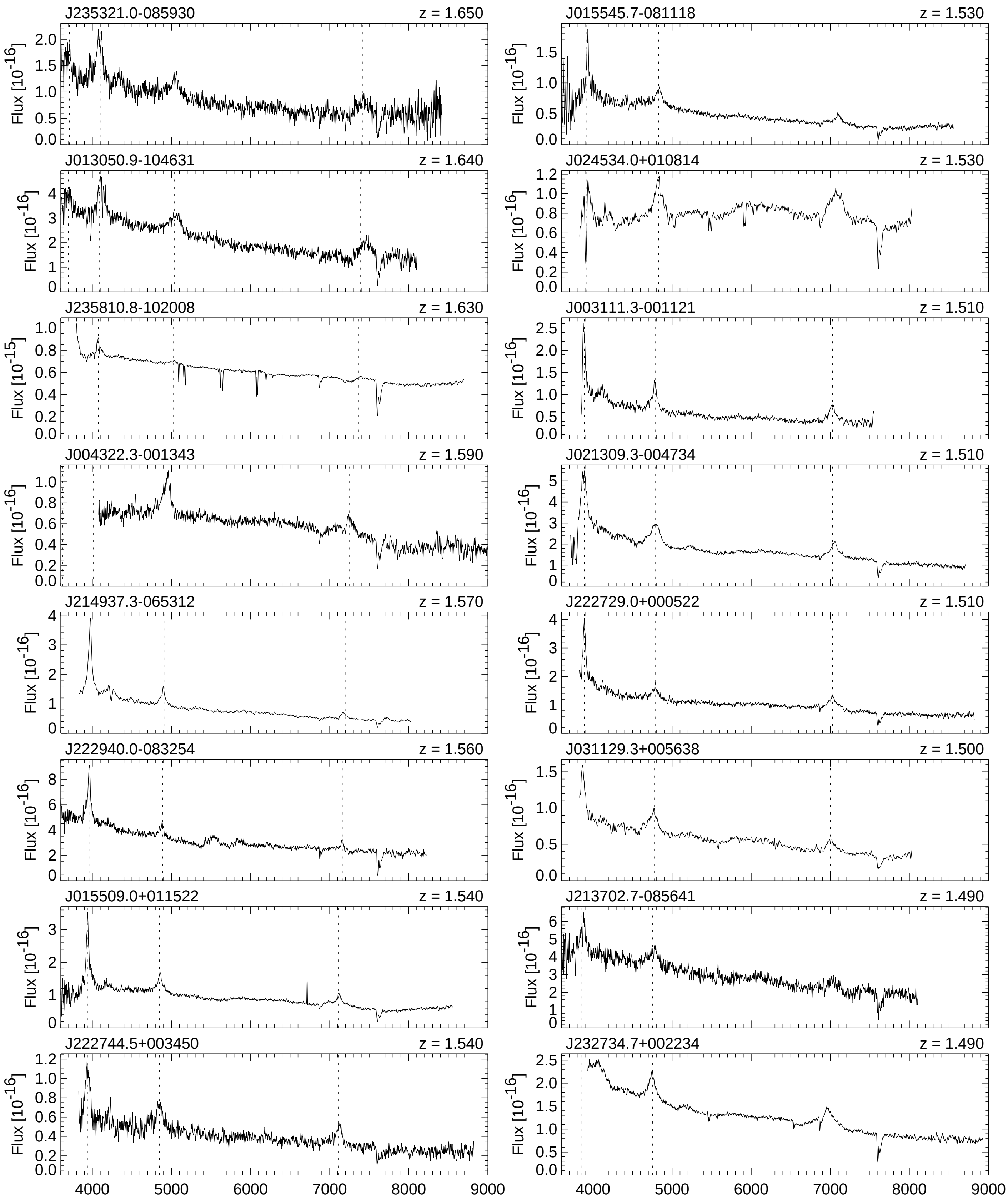

FIG. 9F.— *Continued.* Spectra of FBQS quasars.

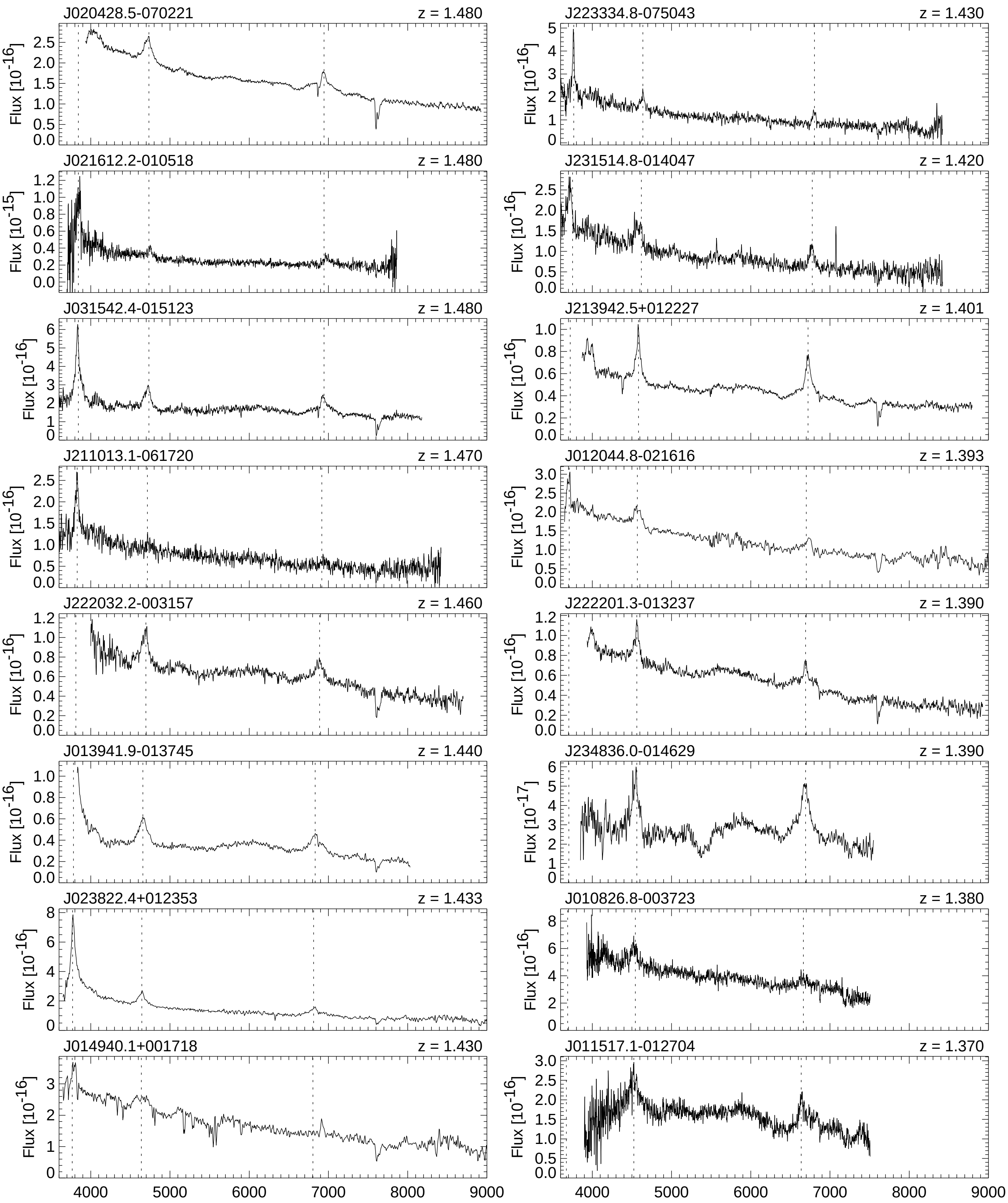

FIG. 9G.— *Continued.* Spectra of FBQS quasars.

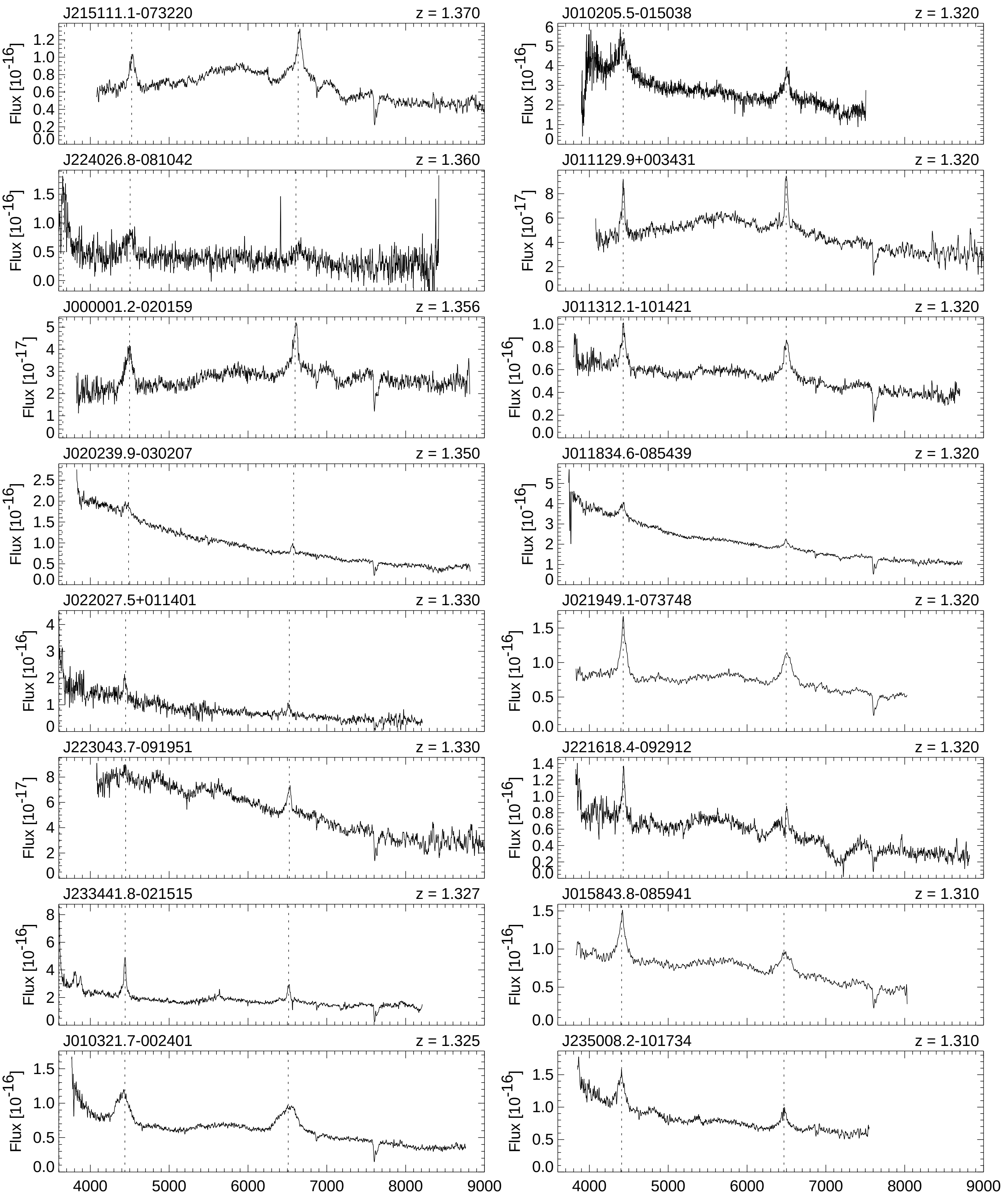

Fig. 9h.— *Continued.* Spectra of FBQS quasars.

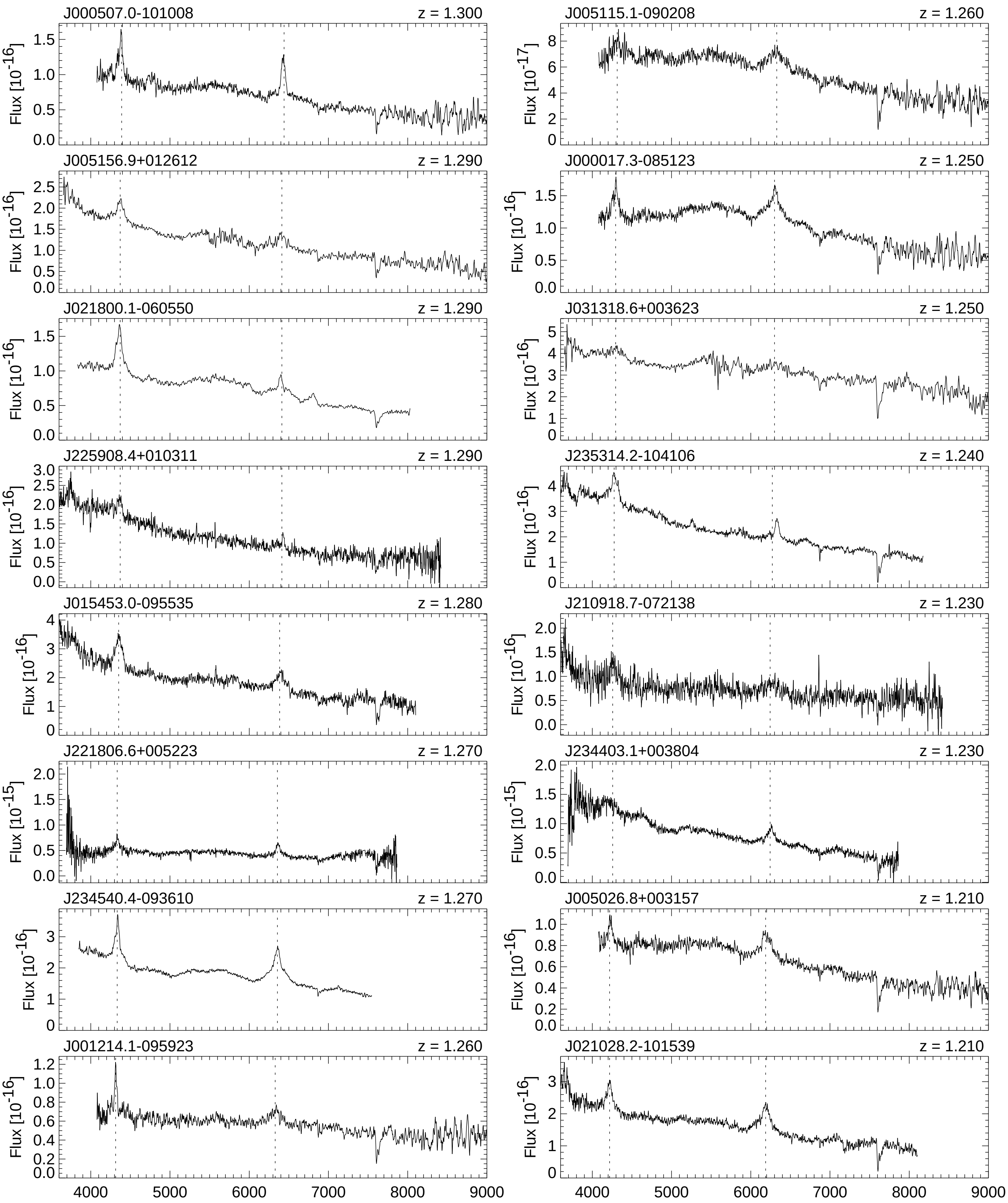

FIG. 9I.— *Continued.* Spectra of FBQS quasars.

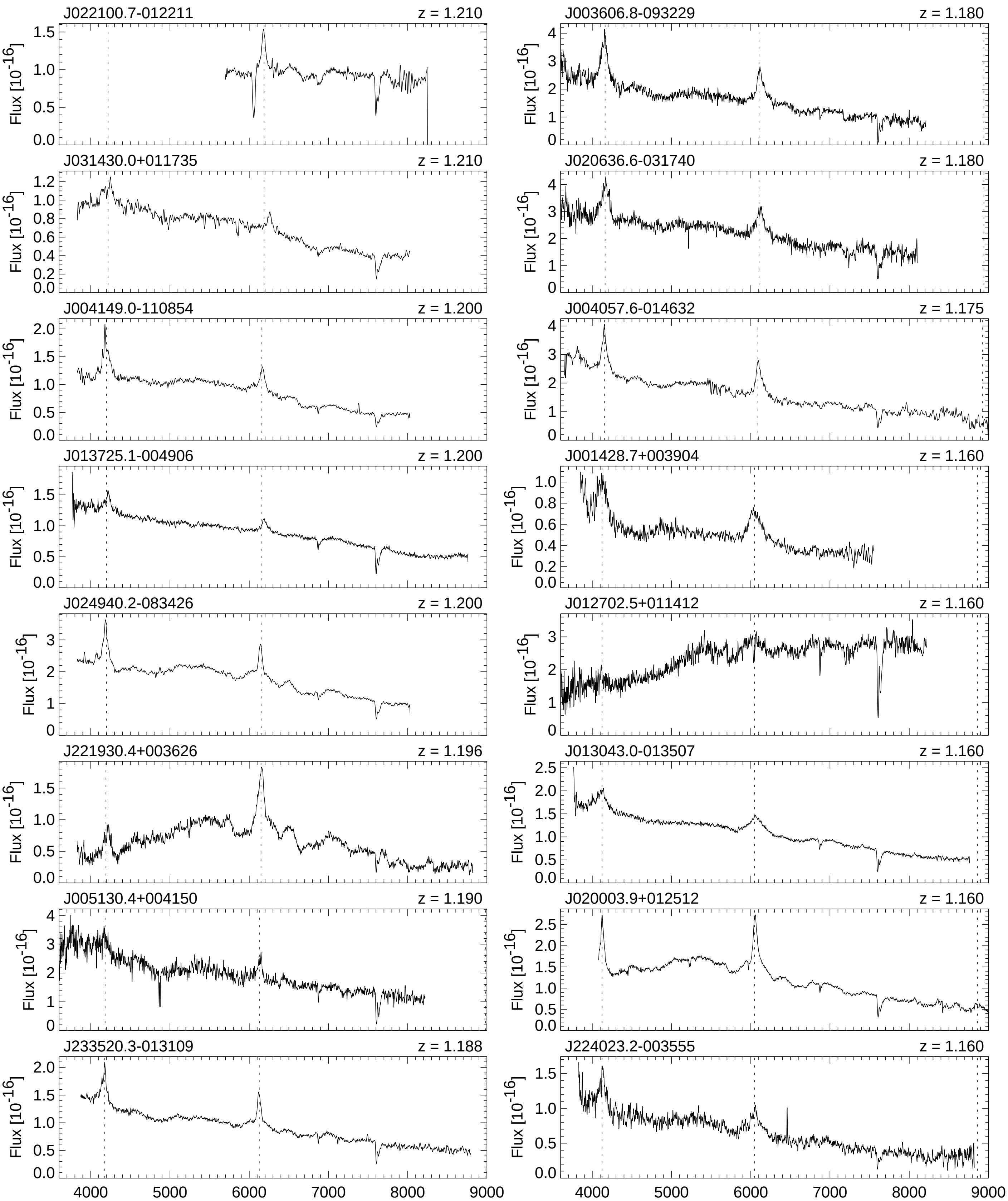

FIG. 9J.— *Continued.* Spectra of FBQS quasars.

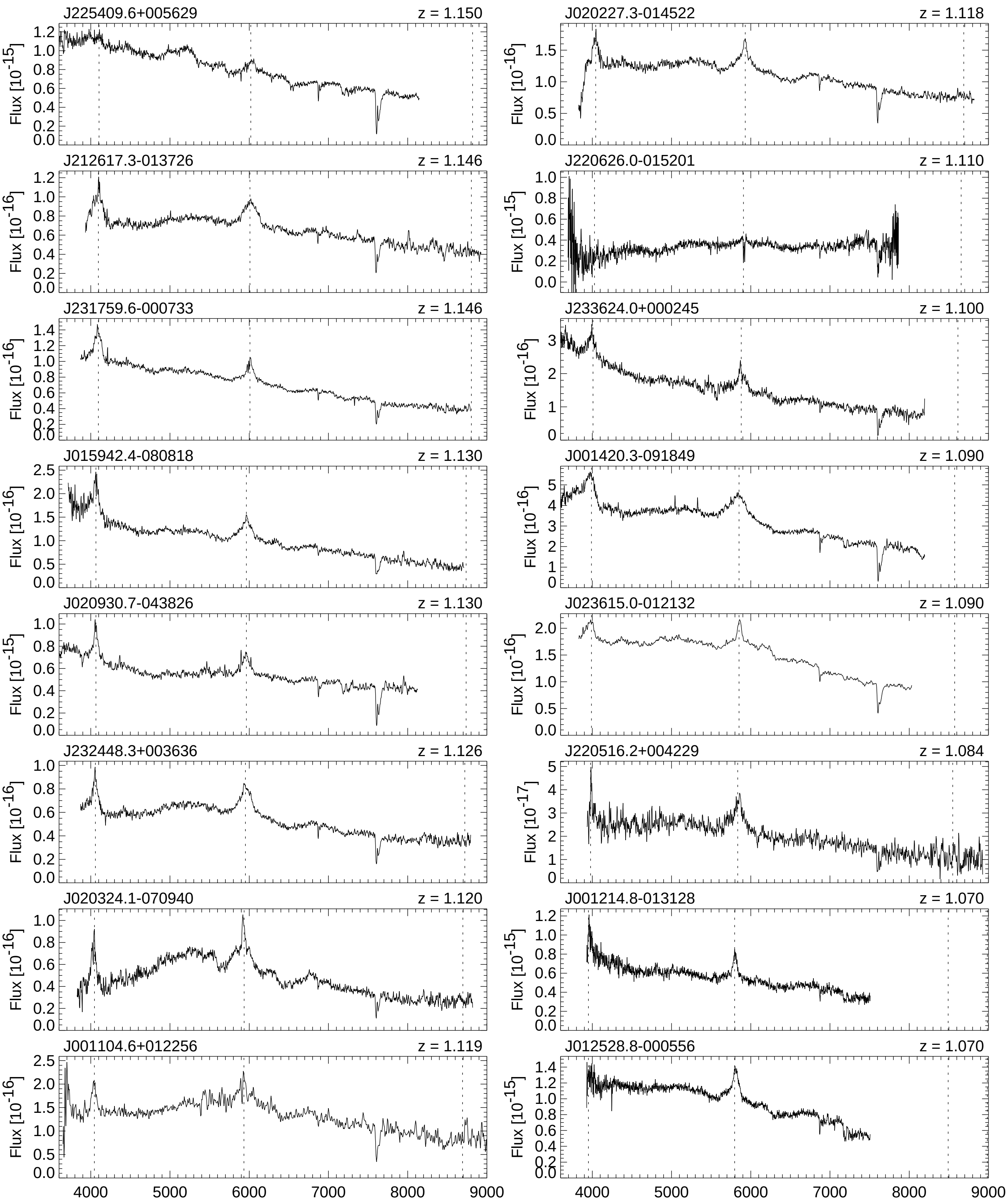

FIG. 9K.— *Continued.* Spectra of FBQS quasars.

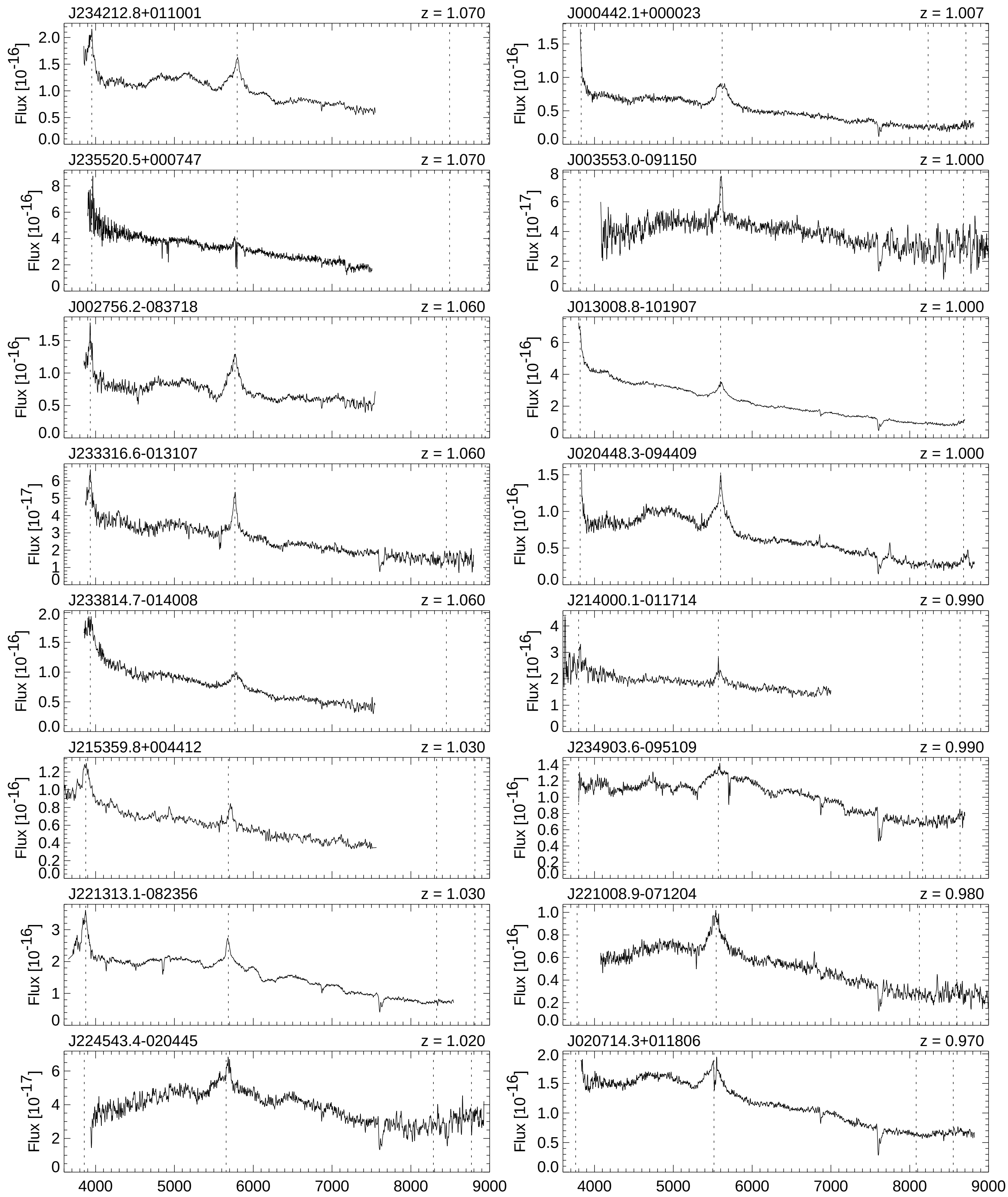

FIG. 9L.— *Continued.* Spectra of FBQS quasars.

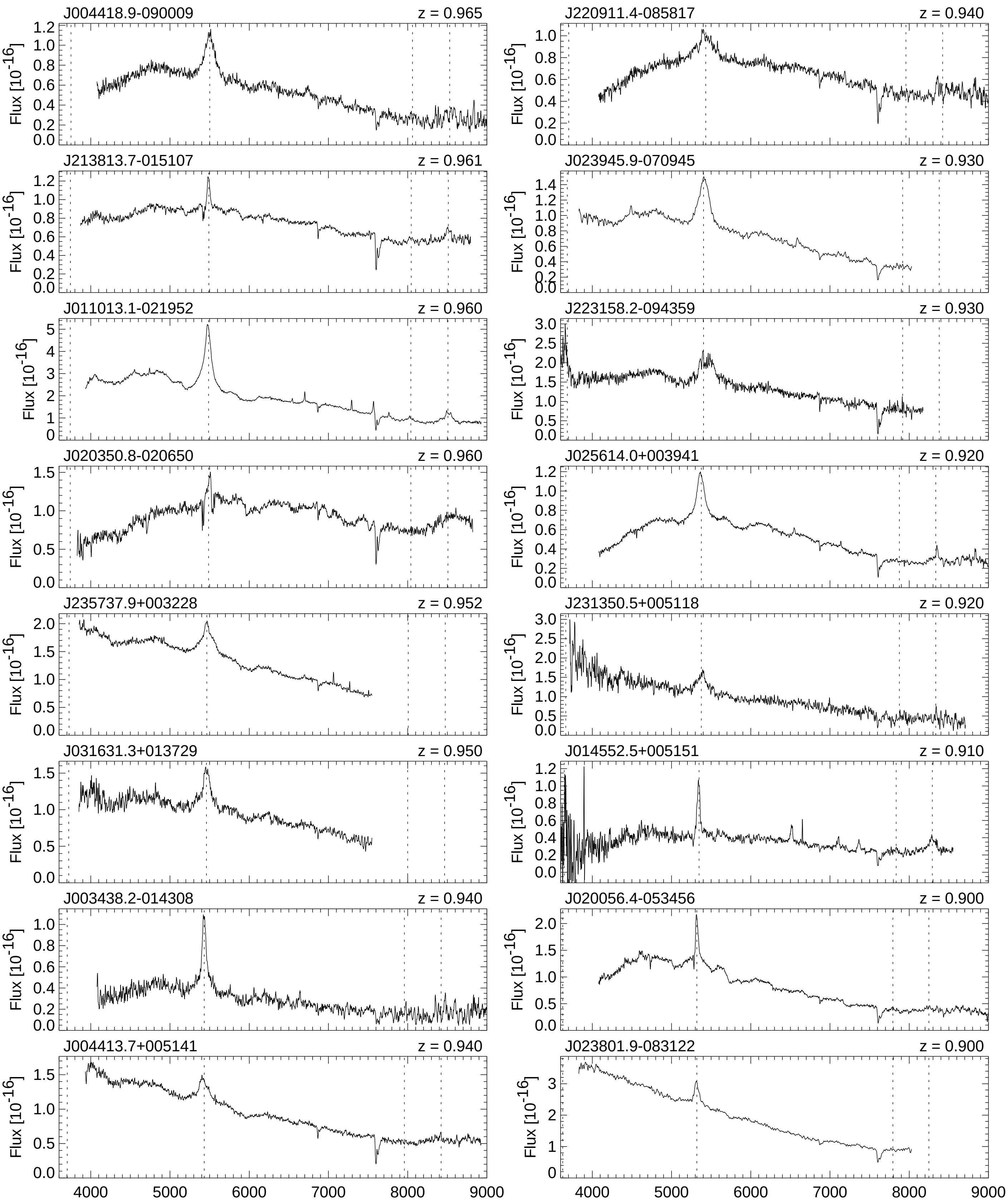

Fig. 9m.— *Continued.* Spectra of FBQS quasars.

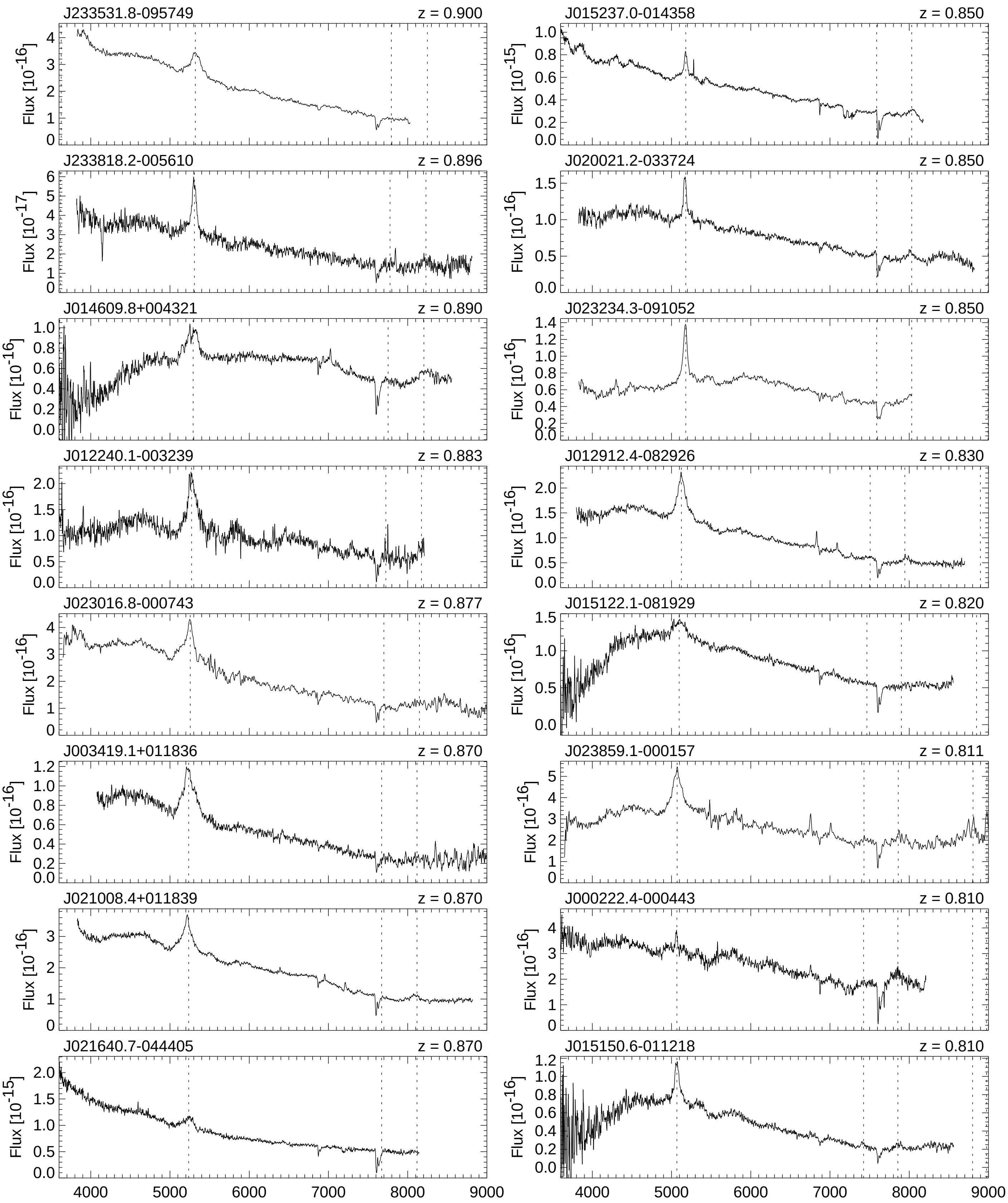

FIG. 9N.— *Continued.* Spectra of FBQS quasars.

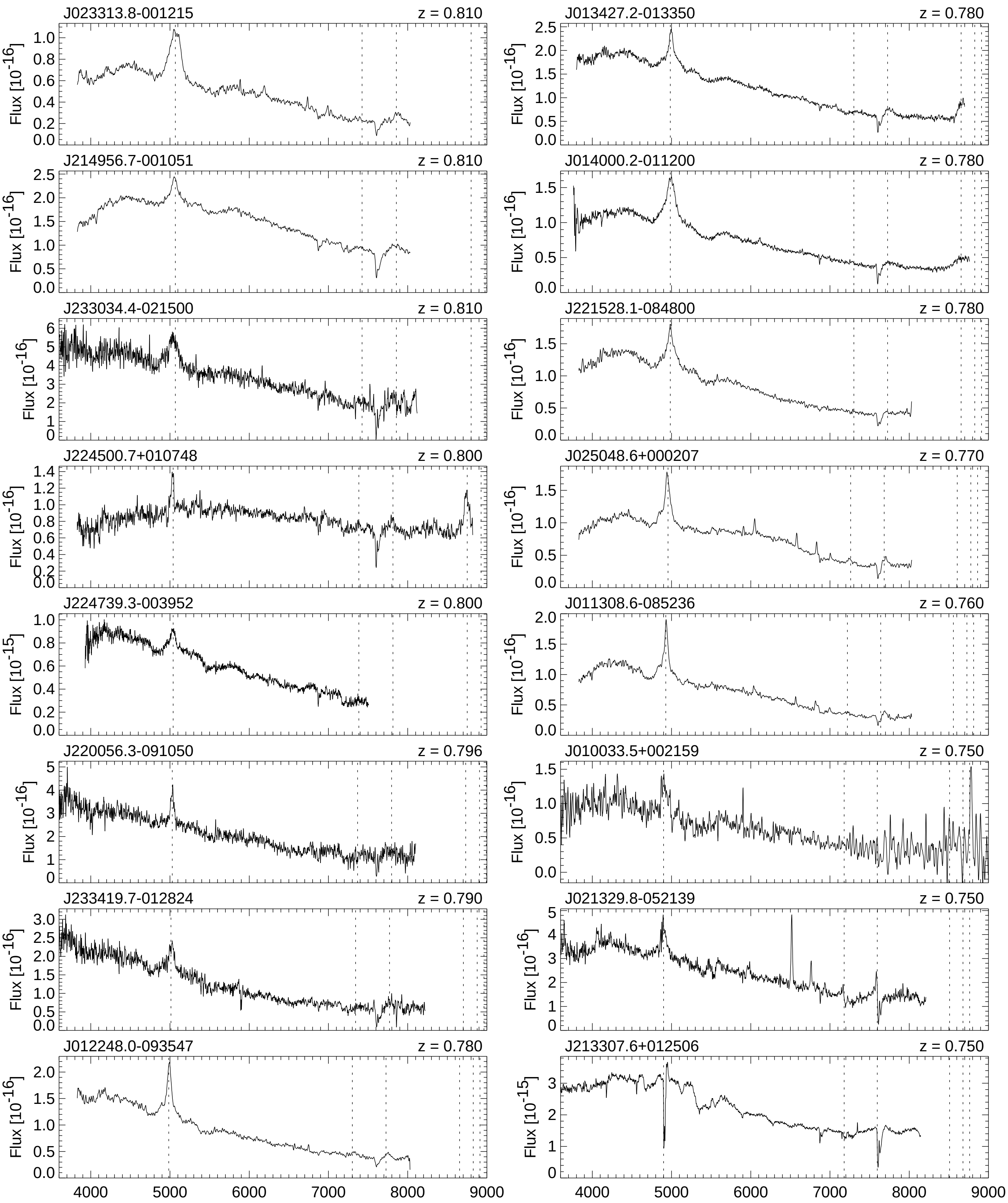

FIG. 90.— *Continued.* Spectra of FBQS quasars.

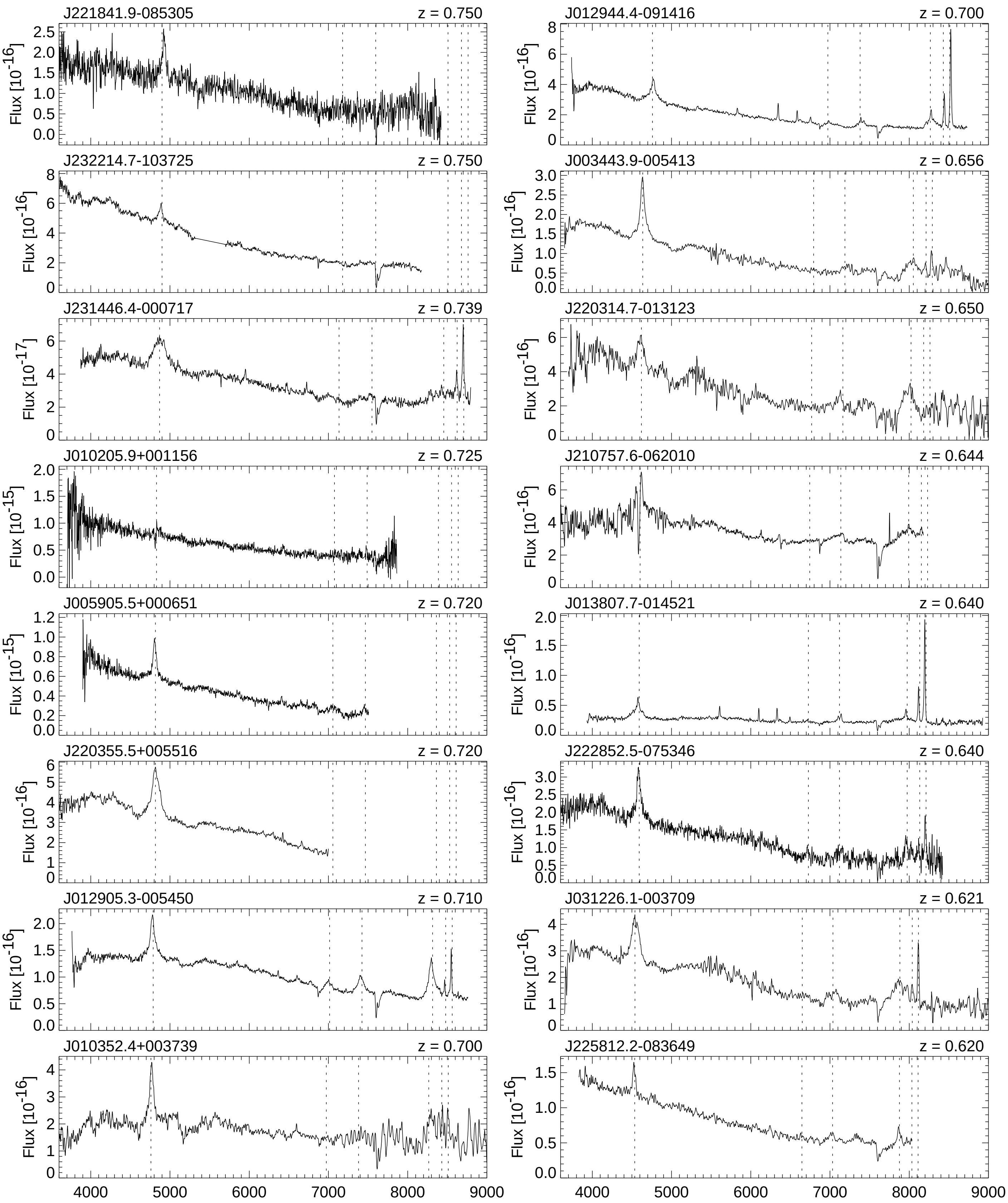

FIG. 9P.— *Continued.* Spectra of FBQS quasars.

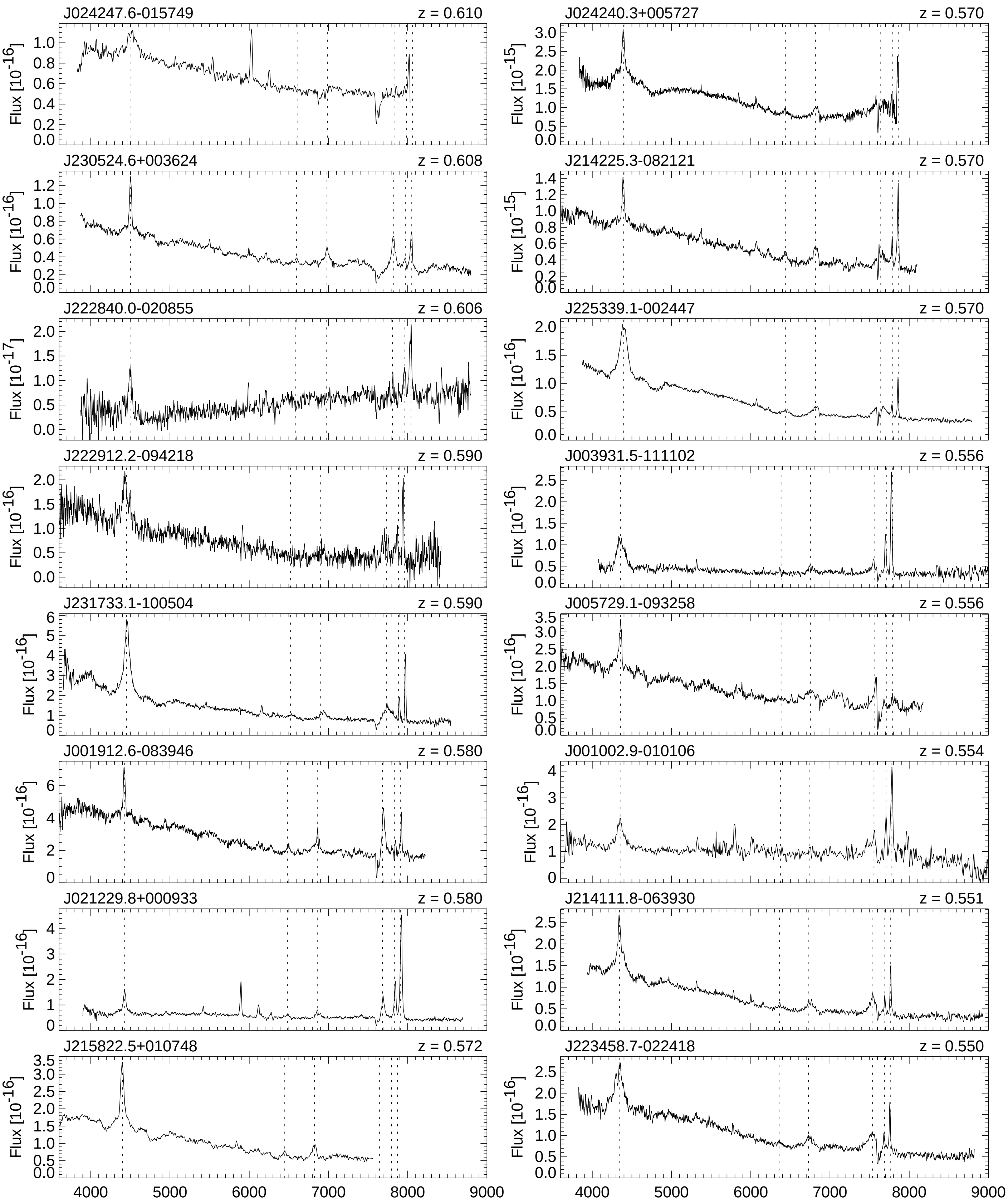

FIG. 9Q.— *Continued.* Spectra of FBQS quasars.

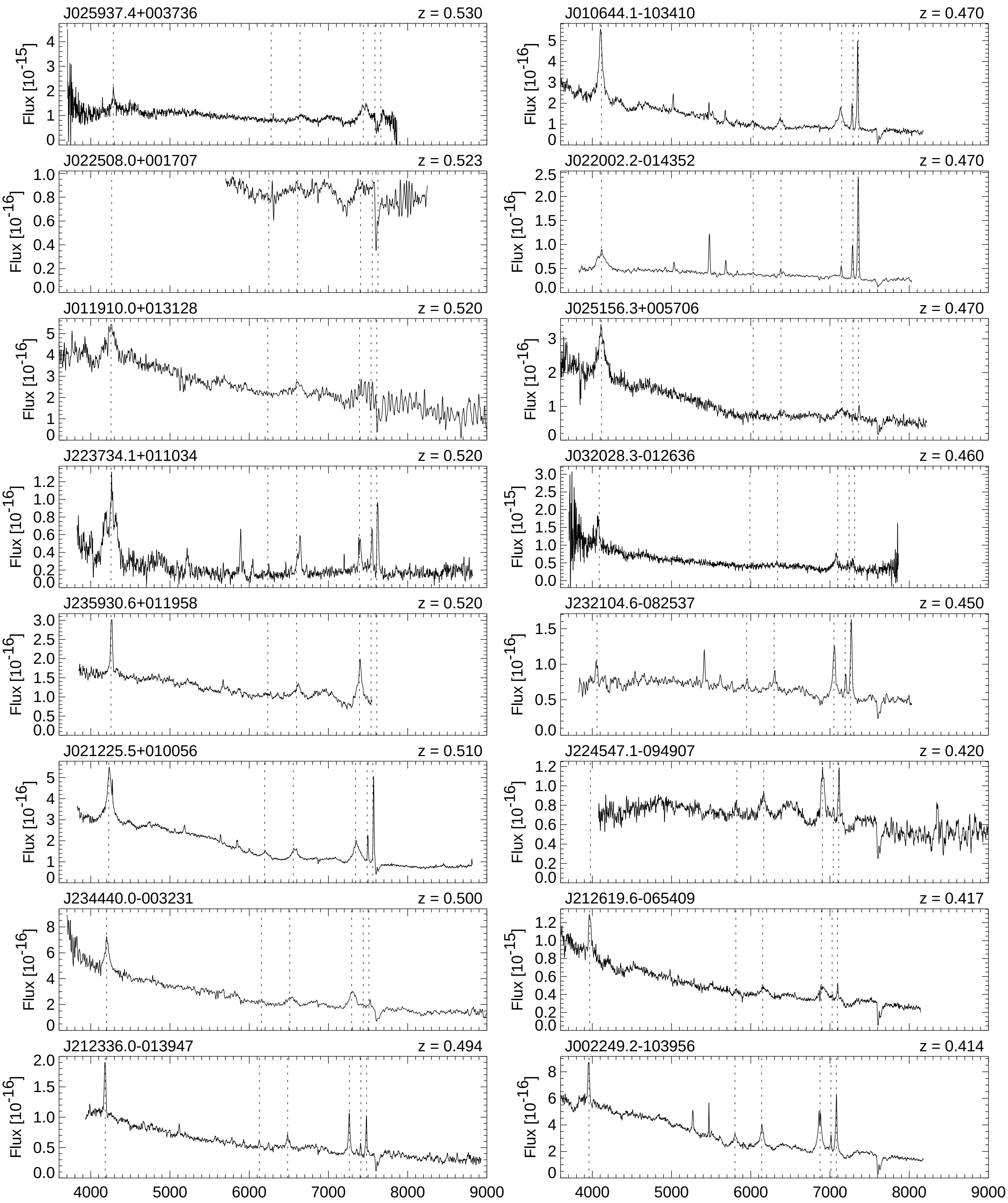

Fig. 9r.— *Continued.* Spectra of FBQS quasars.

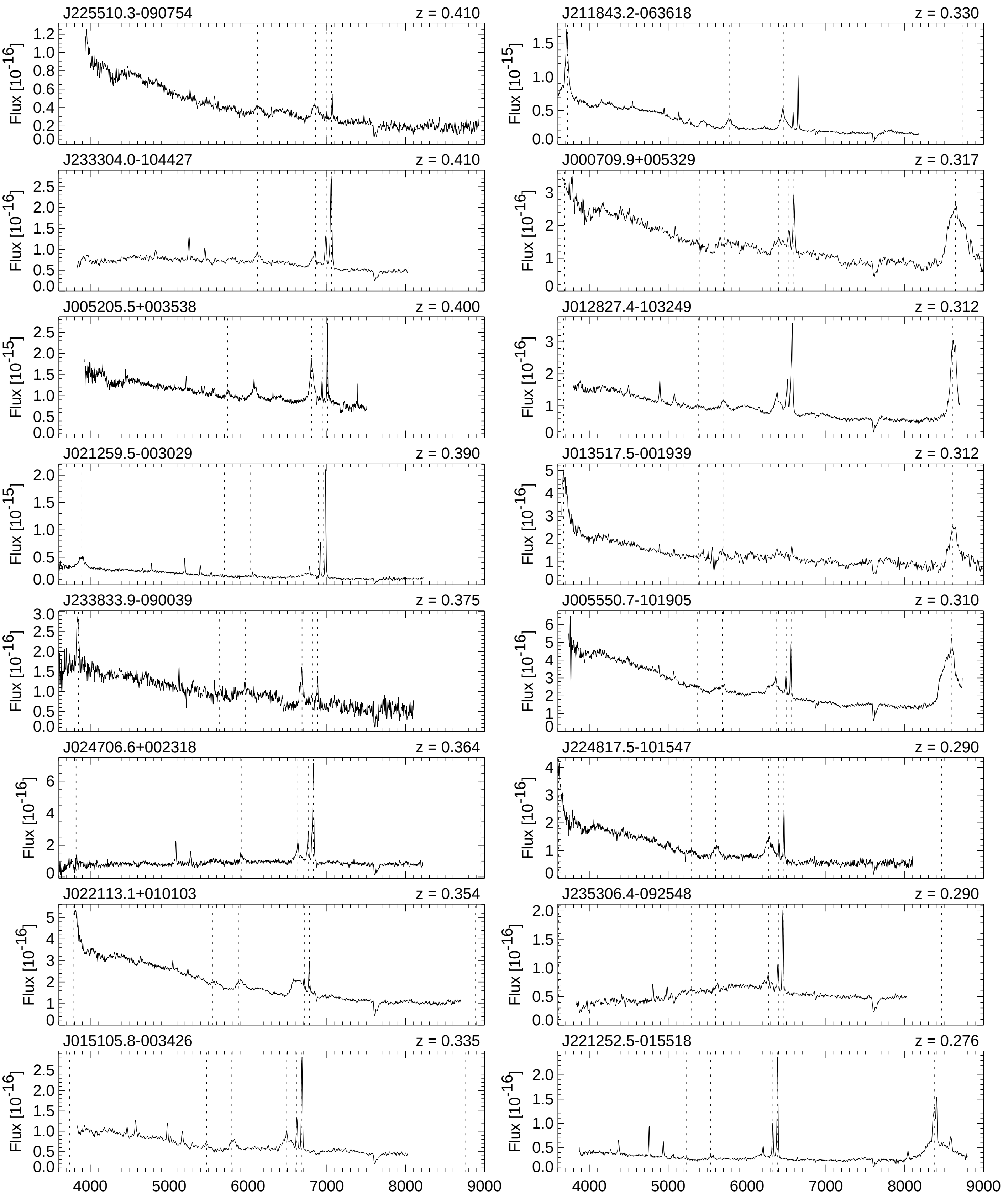

FIG. 9S.— *Continued.* Spectra of FBQS quasars.

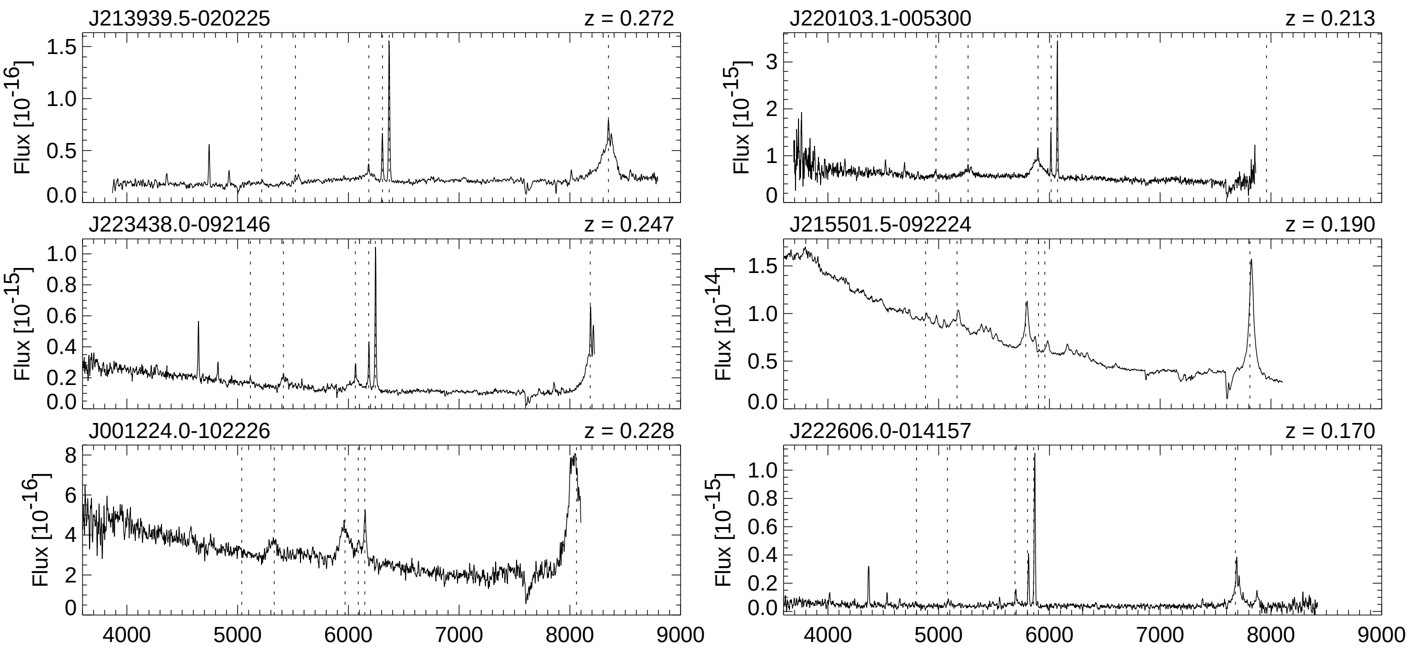

Fig. 9t.— *Continued.* Spectra of FBQS quasars.